Electronic Supplementary Information

Soluble porous carbon cage-encapsulated highly active metal nanoparticle catalysts

Hangyu Liu,[a,b] Liyu Chen,[b] Chun-Chao Hou,[b] Yong-Sheng Wei[b] and Qiang Xu*[a,b]

[a]Research Institute of Electrochemical Energy, National Institute of Advanced Industrial Science and Technology (AIST), Ikeda, Osaka 563-8577, Japan.

[b]AIST-Kyoto University Chemical Energy Materials Open Innovation Laboratory (ChEM-OIL), National Institute of Advanced Industrial Science and Technology (AIST) and Institute for Integrated Cell-Material Sciences (iCeMS), Kyoto University, Yoshida, Sakyo-ku, Kyoto 606-8501, Japan.

***Corresponding Author**

Email: xu.qiang@icems.kyoto-u.ac.jp.

1. Experimental section

Materials.

All chemicals were commercially available and used without further purification. Methanol (Kishida Chemicals Co., Ltd.), ethanol (Kishida Chemicals Co., Ltd.), cetyltrimethyl ammonium bromide (CTAB, Sigma-Aldrich Co. LLC.), polyvinylpyrrolidone K30 (PVP, Viscosity Average Molecular Wt. 30000, Tokyo Chemical Industry Co., Ltd.), Ru/C (Tokyo Chemical Industry Co.), Ru metal powder (Tokyo Chemical Industry Co.), Ru/Al_2O_3 (Wako Pure Chemical Industries), Ru_3CO_{12} (Wako Pure Chemical Industries), zinc nitrate hexahydrate ($Zn(NO_3)_2 \cdot 6H_2O$, Wako Pure Chemical Industries, ≥99.0 %), 2-methylimidazole (Tokyo Chemical Industry Co., >97 %), sodium tetrachloropalladate (Na_2PdCl_4, Tokyo Chemical Industry Co., Ltd.), hydrogen tetrachloroaurate tetrahydrate ($HAuCl_4 \cdot 4H_2O$, Wako Pure Chemical Industries, >95 %), hydrofluoric acid (HF, Wako Pure Chemical Industries, 46 %), hydrochloric acid (HCl, FUJIFILM Wako Pure Chemical Corporation, 35.0-37.0 %), hydrogen peroxide (35 % in Water, Tokyo Chemical Industry Co., Ltd.), tetraethyl orthosilicate (TEOS, Tokyo Chemical Industry Co., Ltd.), ammonia solution (NH_3H_2O, Wako Pure Chemical Industries), hydrogen hexachloroplatinate(IV) hexahydrate ($H_2PtCl_6 \cdot 6H_2O$, Wako Pure Chemical Industries, >98.5 %), ruthenium(III) chloride ($RuCl_3$, Tokyo Chemical Industry Co., Ltd., >95 %), rhodium(III) chloride trihydrate ($RhCl_3 \cdot 3H_2O$, Wako Pure Chemical Industries, >95 %), ammonia borane (JSC Aviabor, purity 97 %) and sodium borohyride ($NaBH_4$, Sigma-Aldrich, 99 %) were used as received.

Synthesis of PVP-capped RuNPs.

In a typical synthesis, $RuCl_3$ (21 mg, 0.1 mmol) and PVP (1111 mg, 10 mmol) were dissolved in 20 mL deionized water and the solution was stirred for 30 min at 0 °C. Then, 5 mL of H_2O solution containing 37 mg of $NaBH_4$ was added into the above solution with vigorous stirring for 2 h. The resulted mixture was dialyzed in water using a dialysis tube (Fraction molecular weight: 3500; Thermo Fisher Scientific K.K.) for 4 h and then was dried in a vacuum oven at 30 °C for 12 h, resulting in the generation of PVP-capped RuNPs.

Synthesis of Ru@Z8.

PVP-capped RuNPs was added into 250 mL methanol containing 2.05 g 2-Melm (25 mmol) followed by ultrasonic treatment for 10 min. Then 90 mg $Zn(NO_3)_2{\cdot}6H_2O$ was pre-added to the above solution. After ultrasonic treatment for another 10 min, the solution was well mixed with 250 mL methanol containing 3.67 g $Zn(NO_3)_2{\cdot}6H_2O$ (12.5 mmol) and kept at room temperature without stirring for 24 h. The product was separated by centrifugation and washed thoroughly with methanol for twice. The resulting powder was then re-dispersed into 40 mL ethanol under long-time ultrasonication for further synthesis of Ru@Z8@SiO_2.

Synthesis of Ru@Z8@SiO_2.

Ru@Z8 was coated with SiO_2 based on a sol-gel process.[1] For the synthesis of Ru@Z8@SiO_2, the above Ru@Z8 dispersion solution was poured into 40 mL ethanol followed by ultrasonic treatment for 4 h. Then 0.6 g CTAB was added to the above solution and a certain amount of ammonia solution was used to adjust pH to 10-11. The mixture was stirred for 12 h. Then 1.5 mL of TEOS was added to the above solution

under vigorous stirring for 24 h. The resulting powder was collected by centrifugation and washed with ethanol for several times. The final product, marked as Ru@Z8@SiO_2 was dried at 30 °C in a vacuum oven for further use.

Synthesis of Ru@ssCC-500.

The as-prepared sample Ru@Z8@SiO_2 was then placed in a ceramic boat and placed into a temperature-programmed furnace under an Ar flow. The temperature was increased to 500 °C at a heating ramp of 2 °C min^{-1} and maintained for 2 h. After cooling down to room temperature naturally, the resultant black carbons were then washed by 1 M HCl and then 12 % HF. The resulting powders were collected by centrifugation and then were poured into 20 mL water, followed by a 30 min ultrasonication treatment, and the supernatant was collected by centrifugation at 12000 rpm for 5 min (repeat 8 times). The supernatants were collected together and the black precipitate disappeared. The Ru@ssCC-500 catalyst was obtained by filtering the supernatants using a 25 nm membrane.

Synthesis of Ru@ssCC-600.

The as-prepared sample Ru@Z8@SiO_2 was then placed in a ceramic boat and placed into a temperature-programmed furnace under an Ar flow. The temperature was increased to 600 °C at a heating ramp of 2 °C min^{-1} and maintained for 2 h. After cooling down to room temperature naturally, the resultant black carbons were then washed by 1 M HCl and then 12 % HF. The resulting powders were collected by centrifugation and then were poured into 20 mL water, followed by a 30 min ultrasonication treatment, and the supernatant was collected by centrifugation at

12000 rpm for 5 min (repeat 8 times). The supernatants (colorless) and residual precipitate were collected. Finally, the precipitate (Ru@ssCC-600) was dried in a vacuum oven at 30 °C overnight.

Synthesis of Ru@CC-X (X represents the pyrolysis temperature).

The as-prepared sample Ru@Z8 was then placed in a ceramic boat and placed into a temperature-programmed furnace under an Ar flow. The temperature was increased to X °C at a heating ramp of 2 °C min^{-1} and maintained for 2 h. After cooling down to room temperature naturally, the resultant black carbons were then washed by 1 M HCl and then 12 % HF. The resulting powders were collected by centrifugation and then were poured into 20 mL water, followed by a 30 min ultrasonication treatment, and the supernatant was collected by centrifugation at 12000 rpm for 5 min (repeat 8 times). The supernatants (colorless) and residual precipitate were collected. Finally, the precipitate (Ru@CC-X) was dried in a vacuum oven at 30 °C overnight.

Synthesis of Ru@CTAB@SiO_2.

The PVP-capped RuNPs was added into a mixed solution containing 5 g CTAB (20 mL ethanol, 100 mL water and 90 mL methanol), followed by a 30 min ultrasonication treatment. Then a certain amount of ammonia solution was used to adjust pH to 10-11. The mixture was stirred for 12 h. Then 5.6 mL of TEOS was added to the above solution under vigorous stirring for 24 h. Finally, the product was centrifuged and washed with ethanol. The final product, marked as Ru@CTAB@SiO_2 was dried at 30 °C in a vacuum oven for further use.[2]

Synthesis of Ru@ssCC-500(CTAB).

The as-prepared sample Ru@CTAB@SiO_2 was then placed in a ceramic boat and placed into a temperature-programmed furnace under an Ar flow. The temperature was increased to 500 °C at a heating ramp of 2 °C min^{-1} and maintained for 2 h. After cooling down to room temperature naturally, the resultant black carbons were then washed by 1 M HCl and then 12 % HF. The resulting powders were collected by centrifugation and then were poured into 20 mL water, followed by a 30 min ultrasonic treatment, and the supernatant was collected by centrifugation at 12000 rpm for 5 min (repeat 8 times). The supernatants (colorless) and residual precipitate were collected. Finally, the precipitate (Ru@ssCC-500(CTAB)) was dried in a vacuum oven at 30 °C overnight.

Synthesis of M@ssCC-500.

The synthesis method is similar to that of Ru@ssCC-500, except that different precursors are used to synthesize PVP-capped MNPs. The precursors of Pt, Pd, Rh and Au were $H_2PtCl_6 \cdot 6H_2O$, Na_2PdCl_4, $RhCl_3 \cdot 3H_2O$ and $HAuCl_4 \cdot 4H_2O$, respectively.

Synthesis of Z8.

2.05 g 2-methylimidazole (25 mmol) was added into 250 mL methanol followed by ultrasonic treatment for 10 min. Then 90 mg $Zn(NO_3)_2 \bullet 6H_2O$ was pre-added to the above solution. After ultrasonic treatment for another 10 min, the solution was well mixed with 250 mL methanol containing 3.67 g $Zn(NO_3)_2 \bullet 6H_2O$ (12.5 mmol) and kept at room temperature without stirring for 24 h. The product was separated by centrifugation and washed thoroughly with methanol for twice. The resulting powder was then re-dispersed into 40 mL ethanol under long-time ultrasonication.

Synthesis of ssCC-500 catalyst.

The synthesis method is similar to that of Ru@ssCC-500, except directly using Z8 as the precursor.

Synthesis of the support-free catalyst (Ru-SP-Free).

In a typical synthesis, 0.1 mmol of $RuCl_3$ was ultrasonically dissolved in 20 mL of H_2O and the solution was stirred for 1 h at 0 °C. Then, 5 mL of H_2O solution containing 37 mg of $NaBH_4$ was added into the above solution with vigorous stirring, resulting in the generation of Ru-SP-Free catalyst.

Synthesis of CTAB-capped RuNPs.

In a typical synthesis, $RuCl_3$ (21 mg, 0.1 mmol) and CTAB (364 mg, 1 mmol) were dissolved in 20 mL deionized water and the solution was stirred for 30 min at 0 °C. Then, 5 mL of H_2O solution containing 37 mg of $NaBH_4$ was added into the above solution with vigorous stirring for 2 h. The resulted mixture was dialyzed in water using a dialysis tube (Fraction molecular weight: 3500; Thermo Fisher Scientific K.K.) for 4 h and then was dried in a vacuum oven at 30 °C for 12 h, resulting in the generation of CTAB-capped RuNPs.

Procedures for the decomposition of H_2O_2.

The as-synthesized catalyst with 2.5 mL of H_2O mixture was carefully poured into a two-necked flask, which was placed in a water bath under ambient atmosphere. A gas burette filled with water was connected to the two-necked flask to collect the generated gas. After 0.52 mL H_2O_2 solution (35 % in Water) was added to the flask, the catalytic reaction started and the yield of generated O_2 was recorded by reading the

volume of the displacement of water in the gas burette. H_2O_2 decomposition was finished when no more gas was generated.

Procedures for the hydrolysis of AB.

The as-synthesized catalyst with 2 mL of H_2O mixture was carefully poured into a two-necked flask, which was placed in a water bath under ambient atmosphere. A gas burette filled with water was connected to the two-necked flask to collect the generated gas. After 1 mL of H_2O solution containing AB (1 mmol) was added to the flask, the catalytic reaction started and the yield of generated H_2 was recorded by reading the volume of the displacement of water in the gas burette. AB hydrolysis was finished when no more gas was generated.

Procedures for the methanolysis of AB.

The as-synthesized catalyst with 2 mL of methanol was carefully poured into a two-necked flask, which was placed in a water bath under ambient atmosphere. A gas burette filled with water was connected to the two-necked flask to collect the generated gas. After 1 mL of methanol solution containing AB (1 mmol) was added to the flask, the catalytic reaction started and the yield of generated H_2 was recorded by reading the volume of the displacement of water in the gas burette. AB methanolysis was finished when no more gas was generated.

Durability test.

The durability testing of Ru@ssCC-500 was performed at 30 °C. The procedure was the same as described in **Procedures for the decomposition of H_2O_2**. After each run, the catalyst was treated with H_2 at 30 °C. Then the catalyst was reused for next cycle.

For each cycle, 0.52 mL of H_2O_2 was injected to the catalysis system. The experiment was repeated for 5 times.

Apparatus and measurements.

The PXRD measurements were carried out using a Rigaku Ultima IV diffractometer with Cu Kα radiation (40 kV, 40 mA). Nitrogen adsorption/desorption isotherms were conducted (77 K) by using an automatic volumetric adsorption equipment (Belsorp-maxII) after activation at 373 K for 12 h under vacuum. Their pore volumes were then calculated by the single-point method (P/P0 = 0.99). X-ray photoelectron spectra (XPS) were carried out on a SHIMADZU ESCA-3400 X-ray photoelectron spectrometer with a Mg Kα source (10 kV, 10 mA). Scanning electron microscopic (SEM) were conducted on a HITACHI scanning electron microscope (Regulus 8220). Inductively coupled plasma-optical emission spectroscopy (ICP-OES, Varian VISTA-MPX) were carried out to analyze the content of metals. The transmission electron microscopic (TEM) and high-annular dark-field scanning TEM (HAADF-STEM) images were collected on TmCCAI G^2 F20 machine with operating voltage at 200 kV equipped with energy-dispersive X-ray detector (EDX). The elemental analysis of carbon, hydrogen and nitrogen elements was performed on MICRO CORDER MT-5 and MT-6 (YANACO Co., Ltd.) instruments. After purging the reactor with nitrogen for three times, the decomposition of H_2O_2 was carried out, and the generated gas was collected, which was analyzed by GC-8A (molecular sieve 5A, Ar as carrier gas) and GC-8A (Porapack N, He as carrier gas) analyzers (Shimadzu). UV-vis spectra were collected on Shimazu UV-2550 spectrophotometer. Thermogravimetric analysis (TGA) was carried out on a Rigaku

Thermo plus EVO2/TG-DTA analyzer. Raman spectra were recorded on a Bruker MultiRAM FT-Raman spectrometer at room temperature with an excitation wavelength of 532 nm. FT-IR analyses were carried out on a Shimadzu IRTracer-100 in ATR mode. XAFS spectra at the Ru K-edge were acquired on beamlines BL11S2 of Aichi Synchrotron Radiation (AichiSR) Center. The storage rings of AichiSR were operated at 1.2 GeV with an approximate current of 300 mA. The data was measured in transmission mode. All spectra were collected under ambient conditions. These acquired EXAFS data were then extracted and processed in accordance with the standard procedures by using ATHENA module implemented in IFEFFIT software packages.[3] The k^2-weighted EXAFS spectra of Ru Kedge were obtained through subtracting their post-edge background from the corresponding overall absorption and subsequently normalizing with reference to the edge-jump step. Then, k^2-weighted $\chi(k)$ data of Ru K-edge were Fourier transformed to the real (R) space by using a hanning windows (d_k = 1.0 $Å^{-1}$) to separate these EXAFS contributions from the different coordination shells. EXAFS wavelet transforms were calculated with the Morlet wavelet.[4]

2. Characterization and performance section

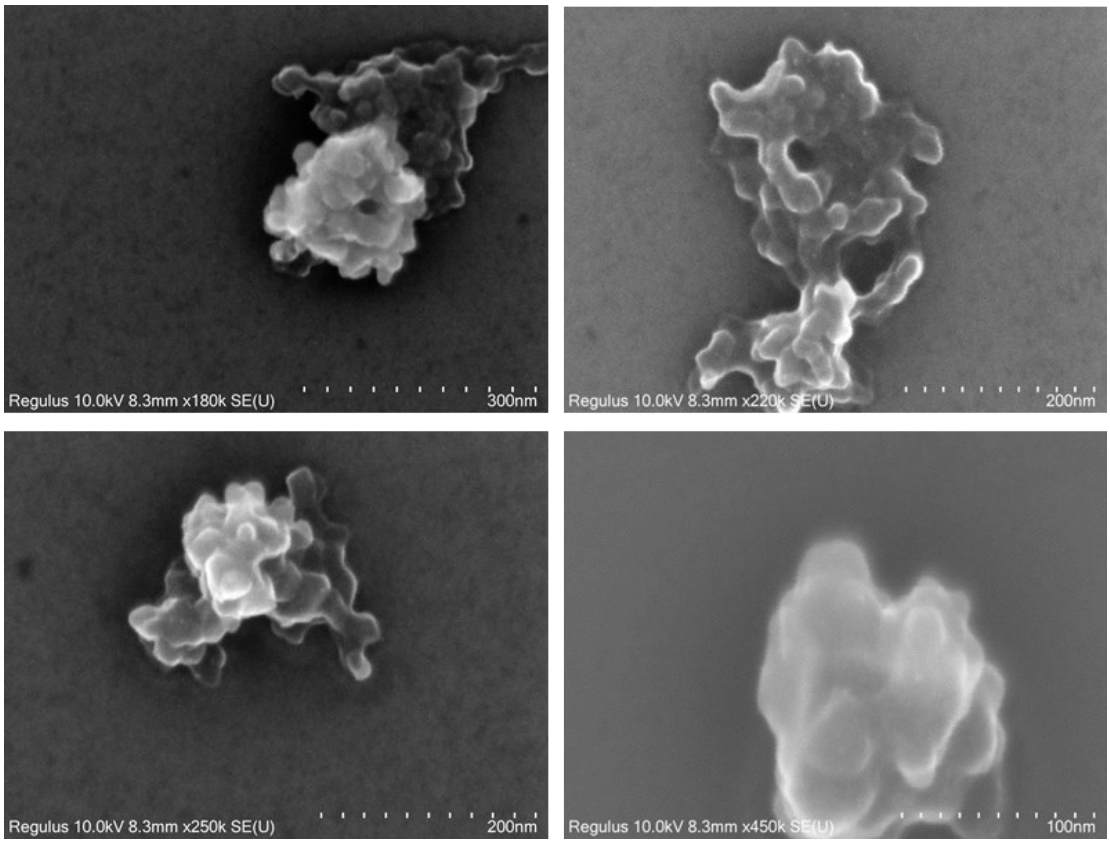

Fig. S1. SEM images of Ru@Z8.

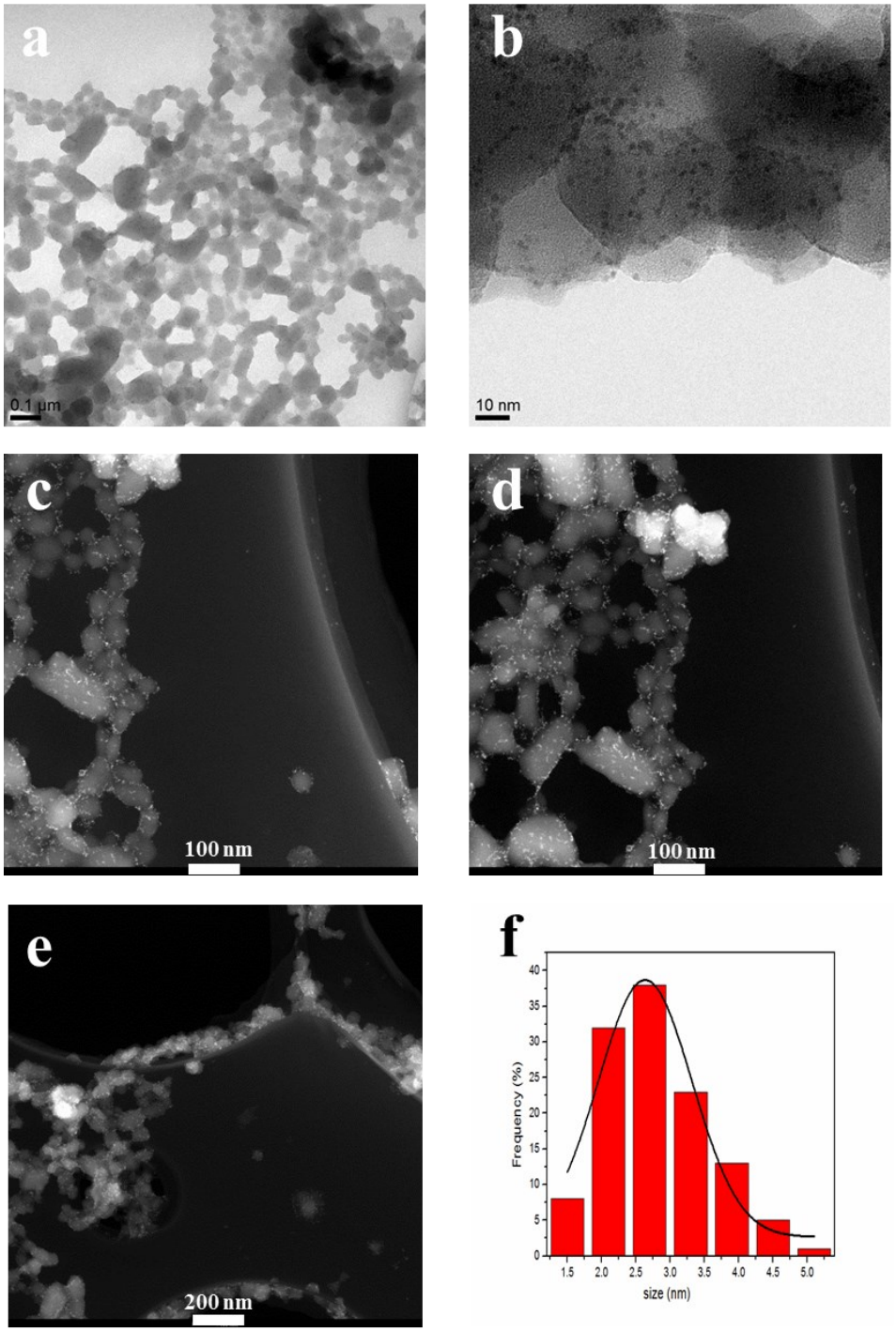

Fig. S2. (**a, b**) TEM, (**c-e**) HAADF-STEM images and (**f**) particle size distribution histogram of the Ru nanoparticles on Ru@Z8.

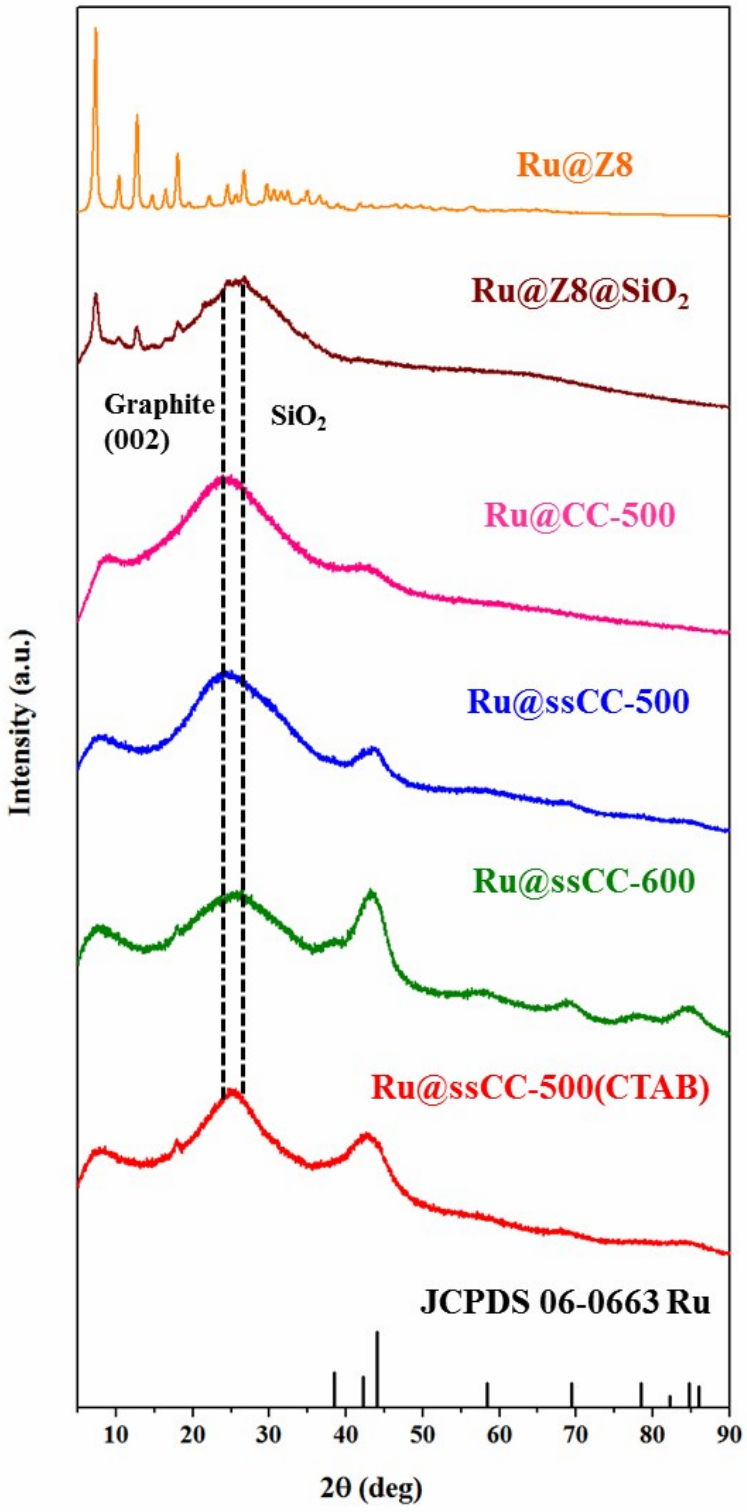

Fig. S3. PXRD patterns of Ru@Z8, Ru@Z8@SiO_2, Ru@CC-500, Ru@ssCC-500, Ru@ssCC-600 and Ru@ssCC-500(CTAB).

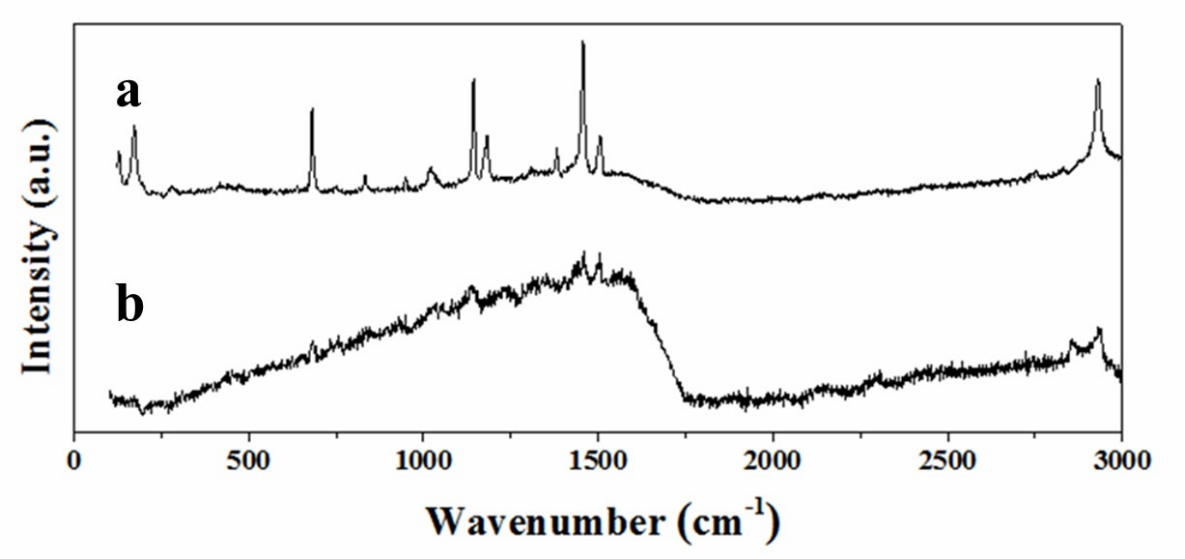

Fig. S4. Raman spectra of (**a**) Ru@Z8 and (**b**) Ru@Z8@SiO_2.

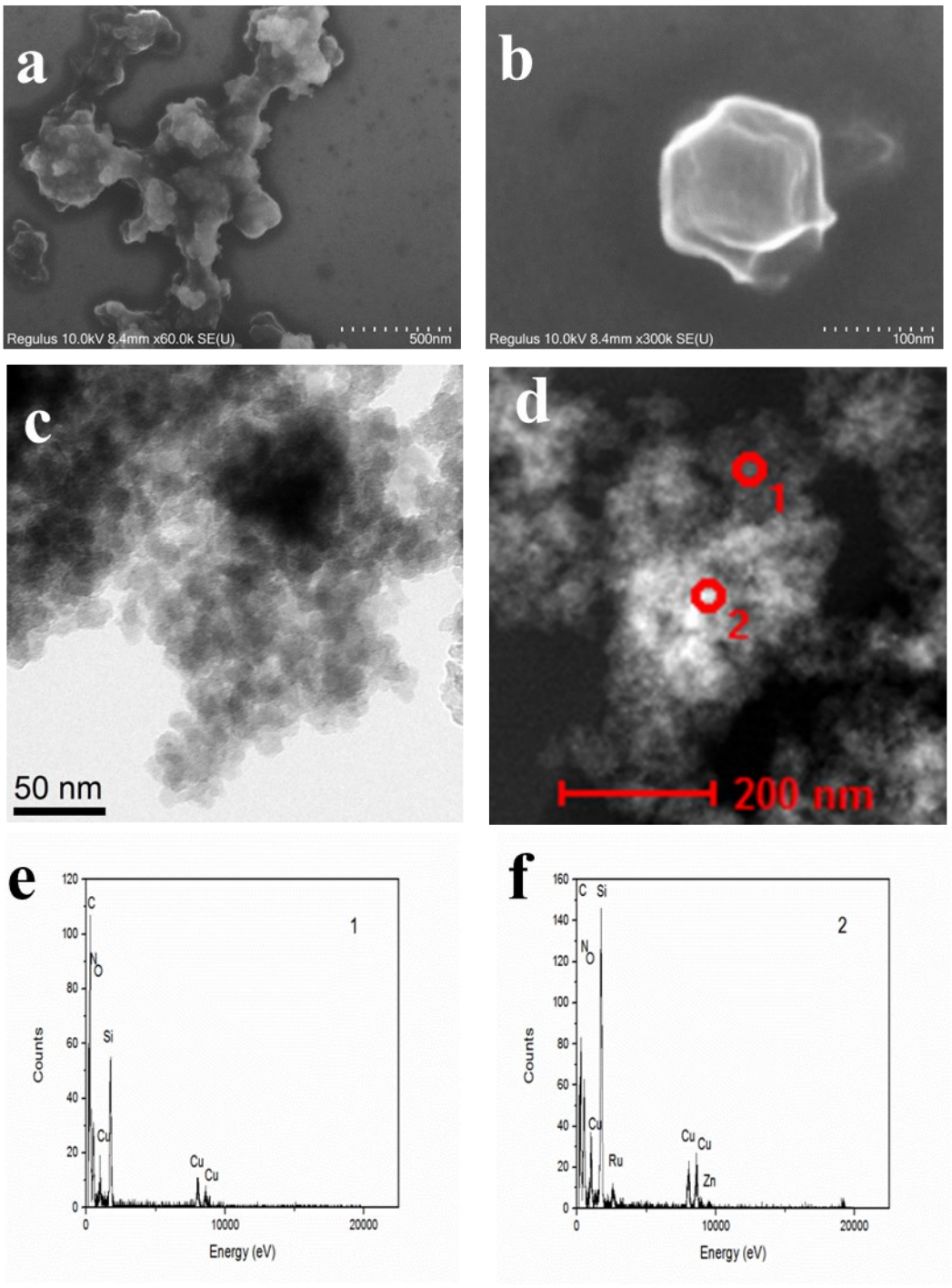

Fig. S5. (**a**, **b**) SEM, (**c**) TEM and (**d**) HAADF-STEM images of Ru@Z8@SiO_2. (**e, f**) EDX patterns of the selected areas (**e**) 1 and (**f**) 2 in (**d**).

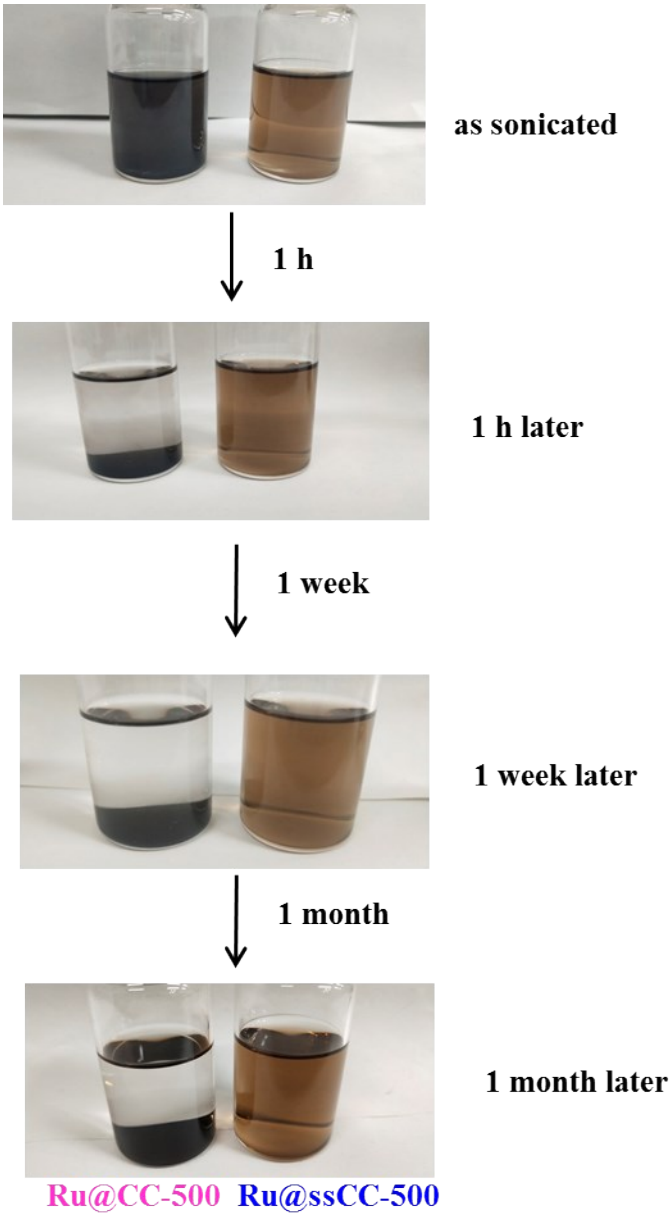

Fig. S6. Photographs of Ru@CC-500 and Ru@ssCC-500 dispersed in ethanol as sonicated and after different durations of sitting.

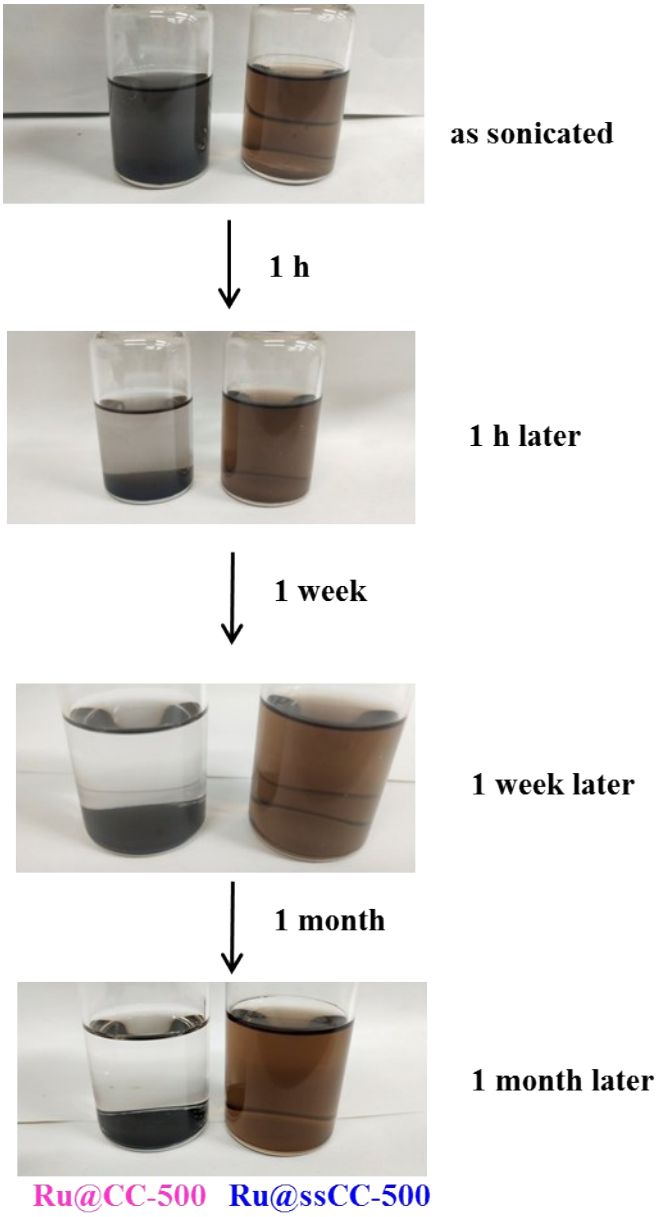

Fig. S7. Photographs of Ru@CC-500 and Ru@ssCC-500 dispersed in methanol as sonicated and after different durations of sitting.

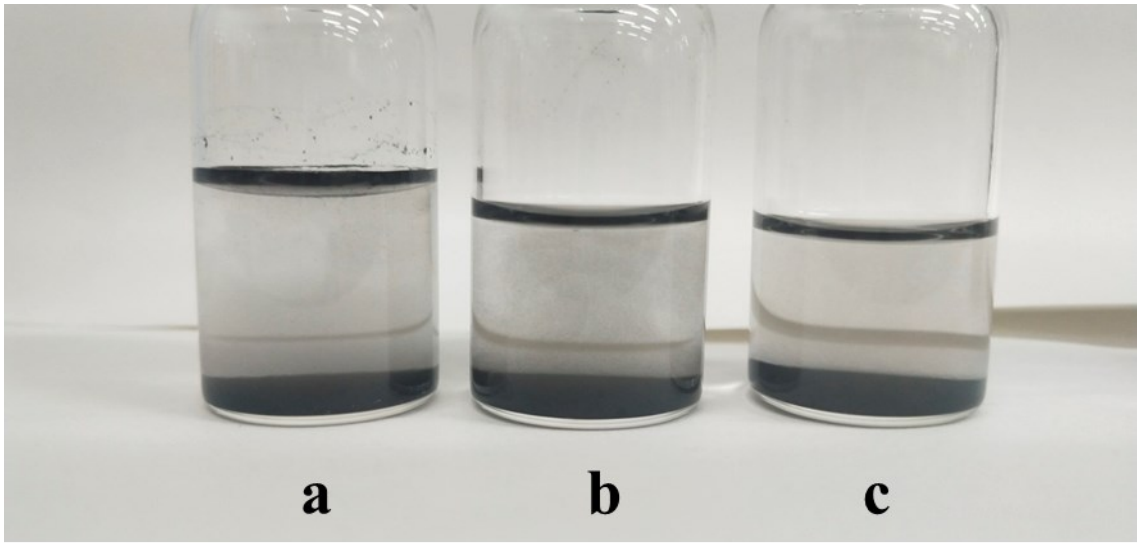

Fig. S8. Photographs of the Ru@ssCC-600 catalyst in (**a**) water, (**b**) ethanol and (**c**) methanol.

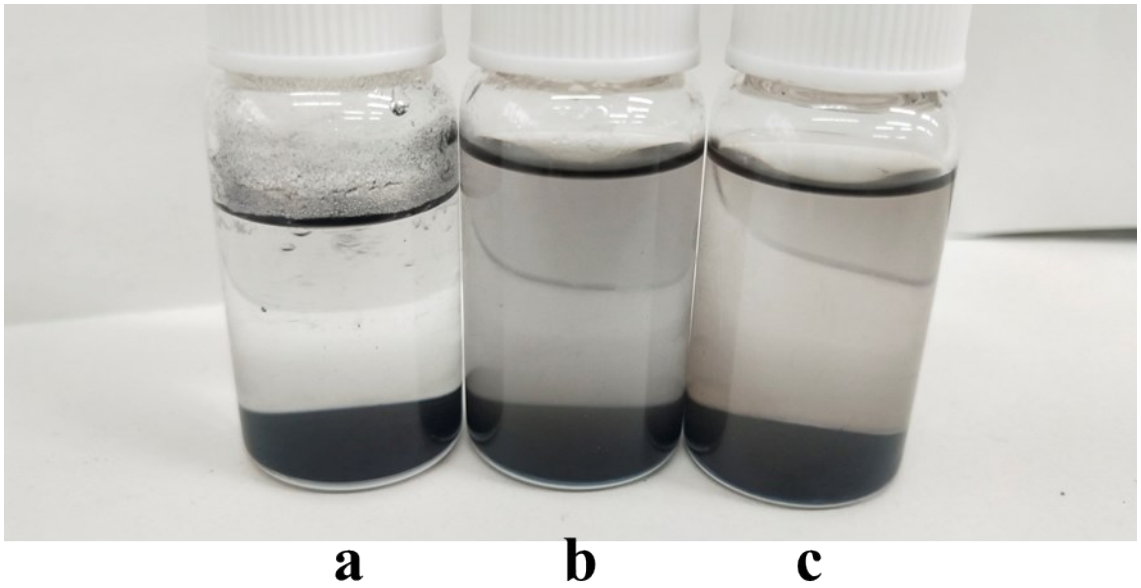

Fig. S9. Photographs of the Ru@CC-600 catalyst in (**a**) water, (**b**) ethanol and (**c**) methanol.

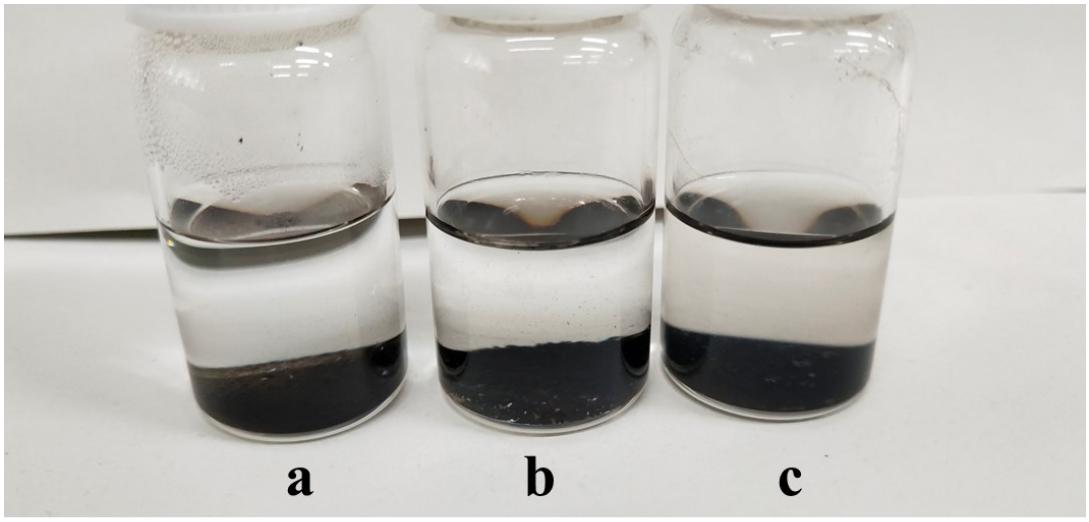

Fig. S10. Photographs of the Ru@ssCC-500(CTAB) catalyst in (**a**) water, (**b**) ethanol and (**c**) methanol.

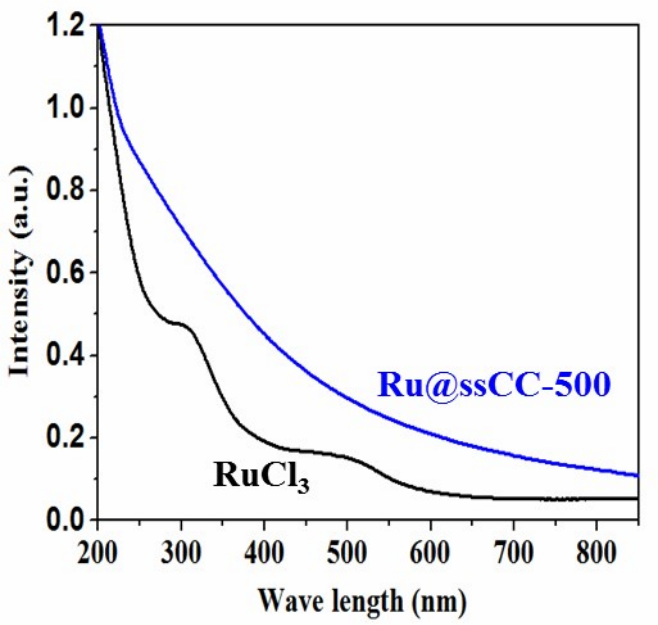

Fig. S11. UV-vis absorption spectra of Ru@mCC-500 and $RuCl_3$ ($n_{(Ru)}$ = 0.0008 mmol) in 4 mL of water. Two peaks appear in the ultraviolet absorption spectrum of $RuCl_3$ solution, which are not observed for Ru@ssCC-500, indicating that Ru^{3+} does not reside in Ru@ssCC-500.

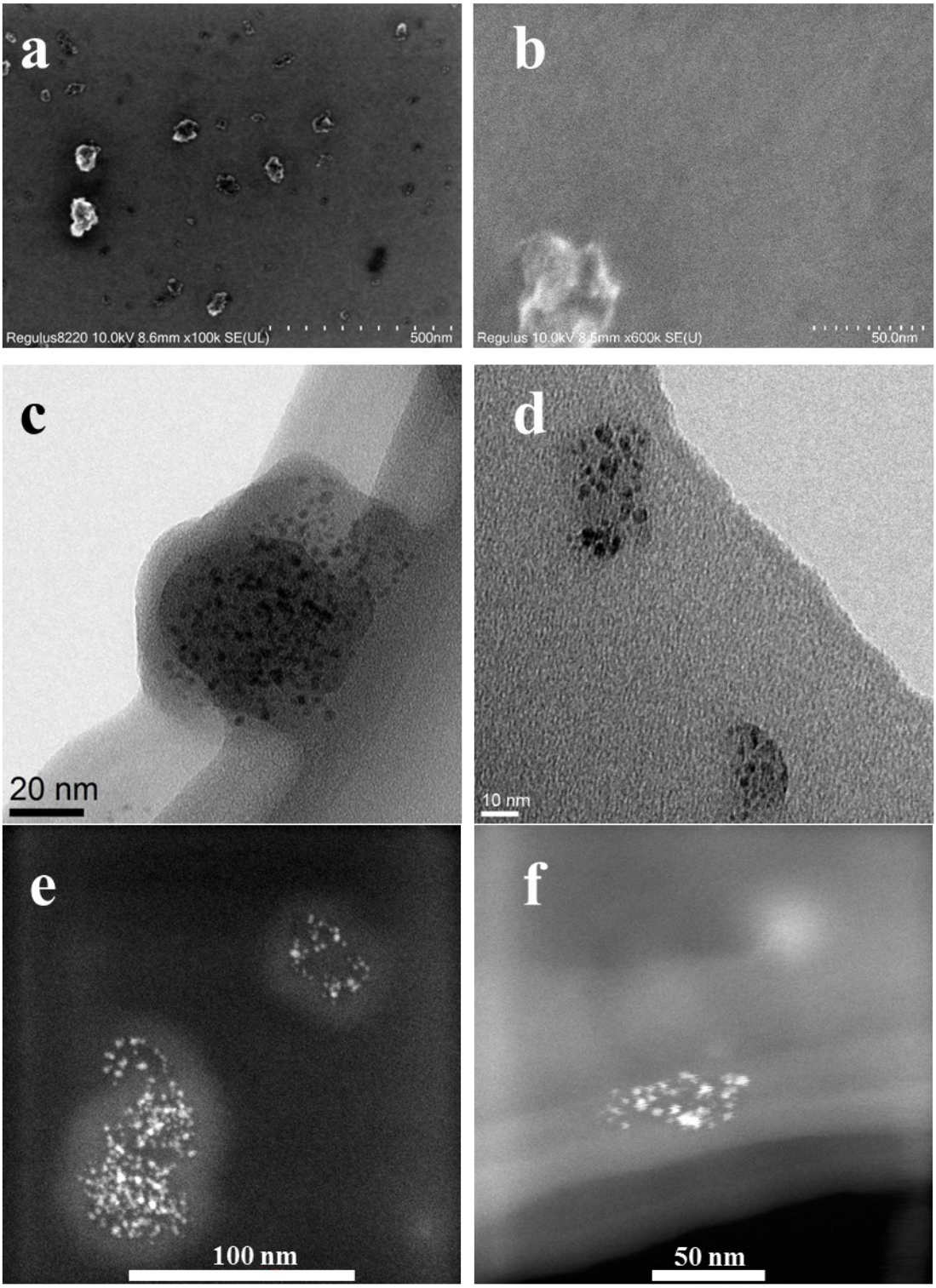

Fig. S12. (**a, b**) SEM, (**c, d**) TEM and (**e, f**) HAADF-STEM images of the Ru@ssCC-500 catalyst.

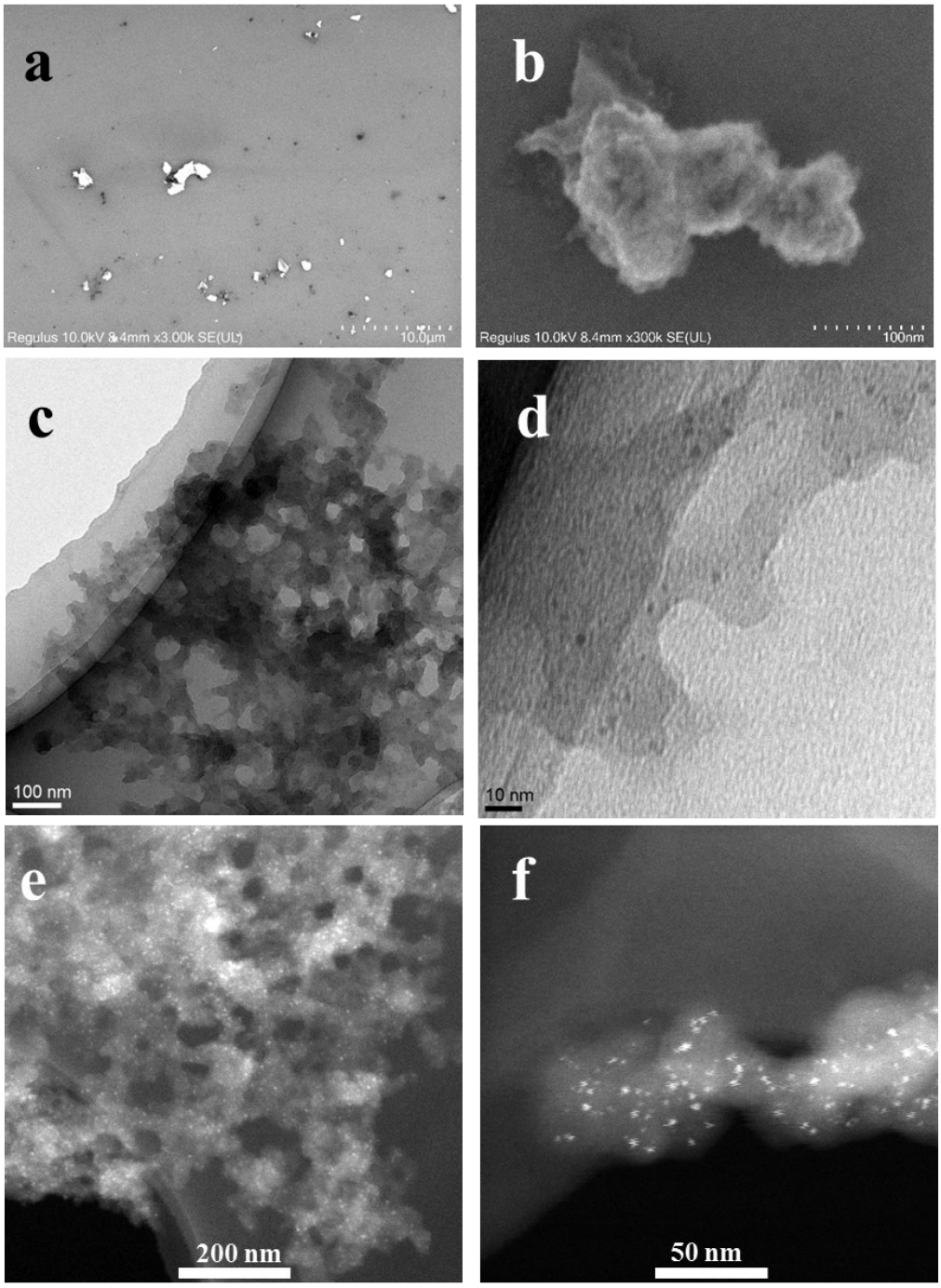

Fig. S13. (**a, b**) SEM, (**c, d**) TEM and (**e, f**) HAADF-STEM images of the Ru@CC-500 catalyst.

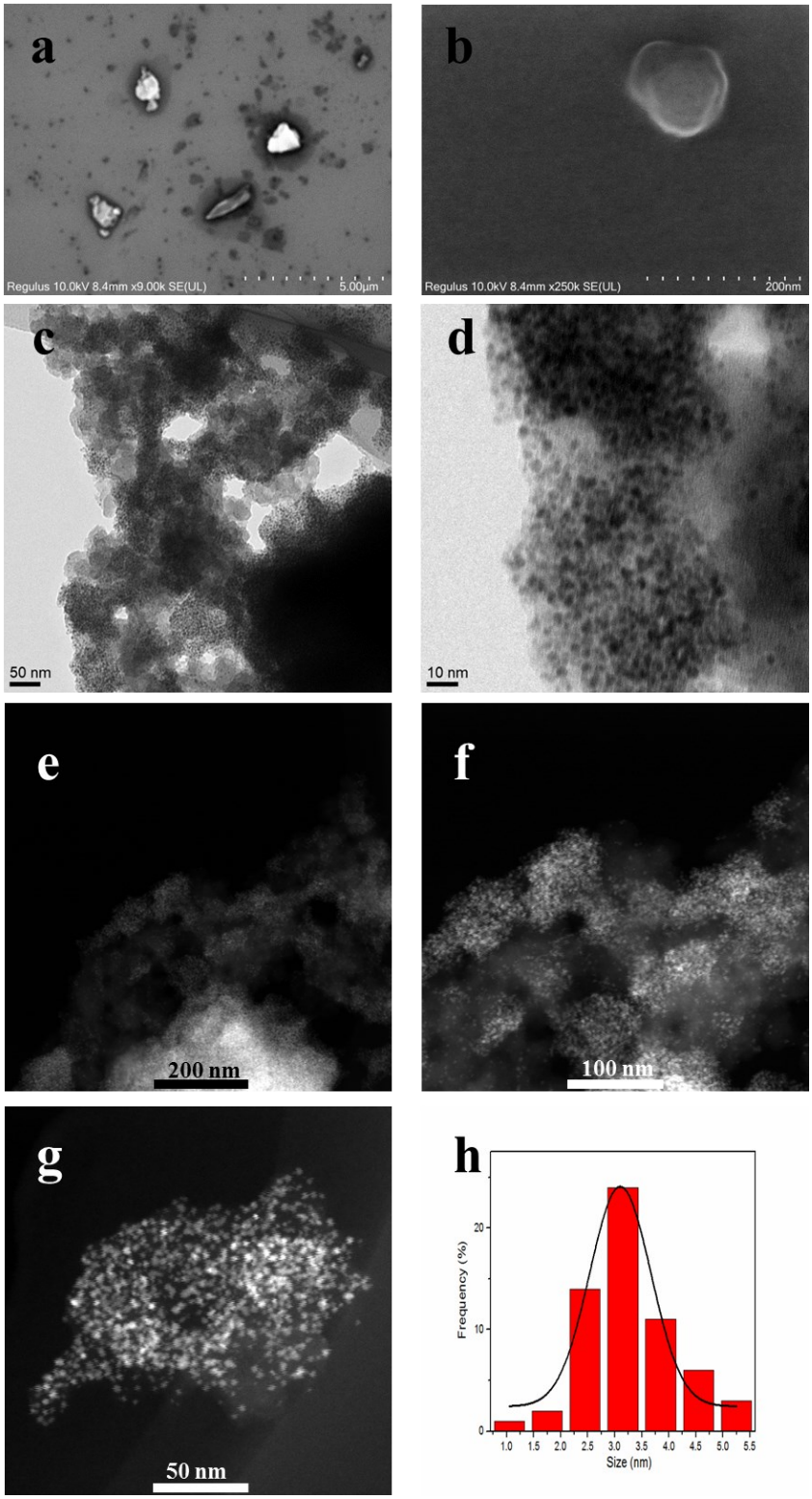

Fig. S14. (**a, b**) SEM, (**c, d**) TEM, (**e-g**) HAADF-STEM images and (**h**) particle size distribution histogram of the Ru nanoparticles on the Ru@ssCC-600 catalyst.

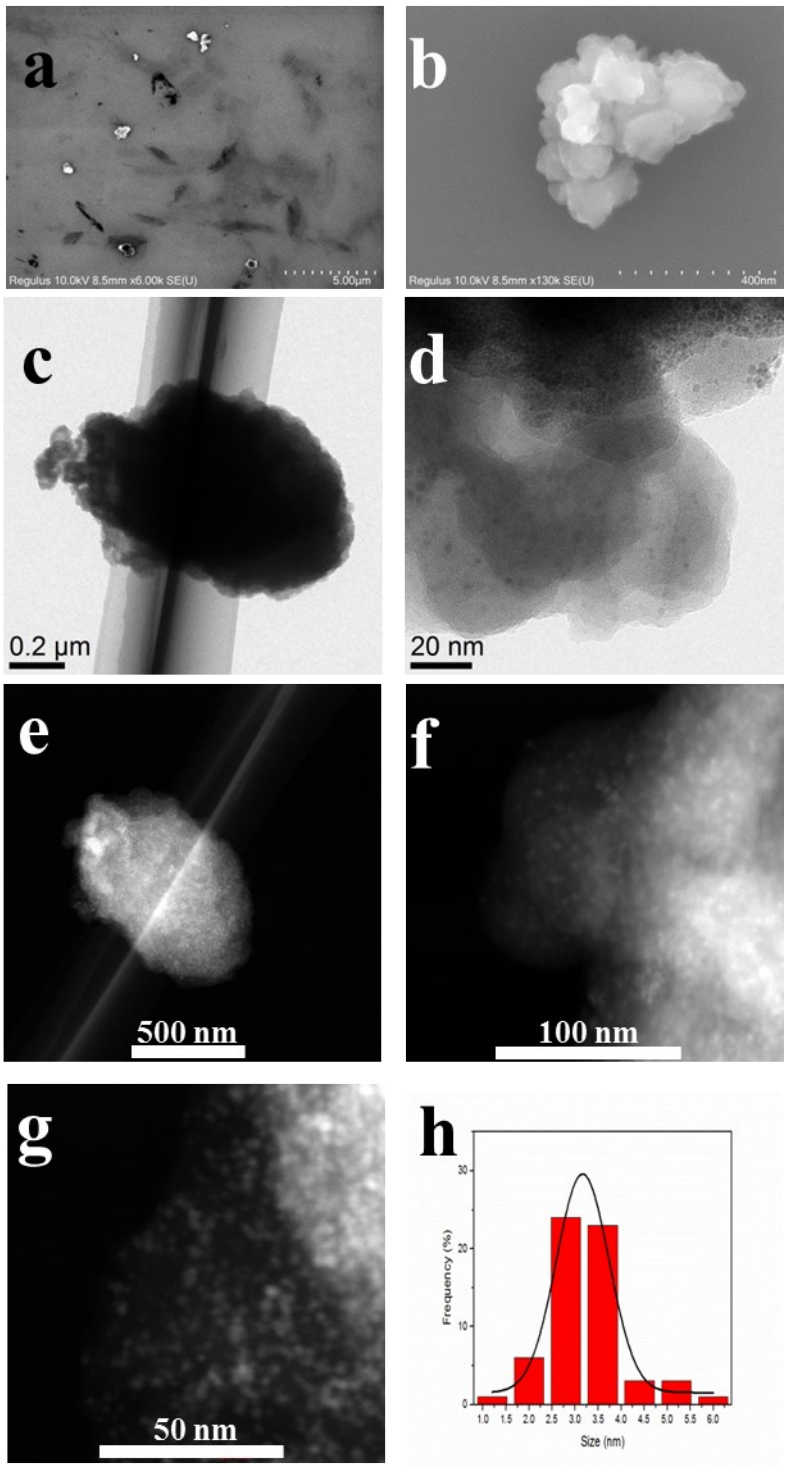

Fig. S15. (**a, b**) SEM, (**c, d**) TEM, (**e-g**) HAADF-STEM images and (**h**) particle size distribution histogram of the Ru nanoparticles on Ru@ssCC-500(CTAB) catalyst.

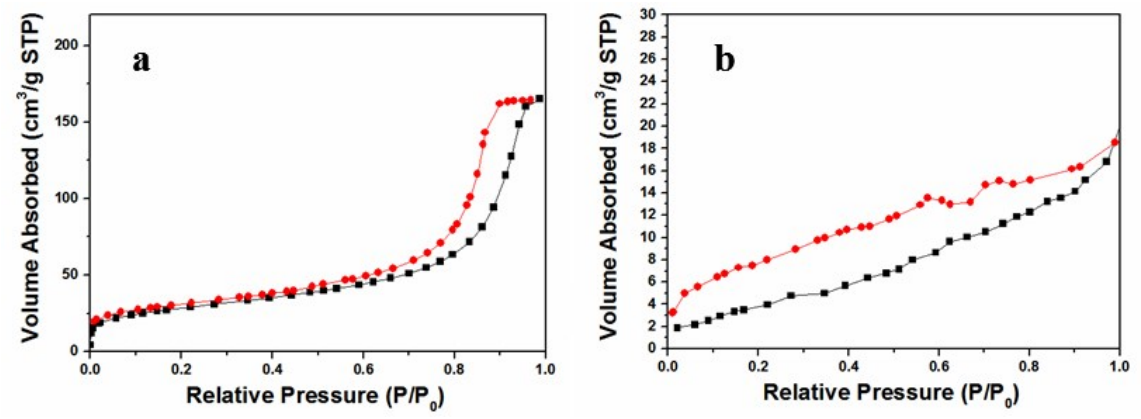

Fig. S16. N_2 sorption isotherms of the (**a**) Ru@CC-500 and (**b**) Ru@ssCC-500 catalysts.

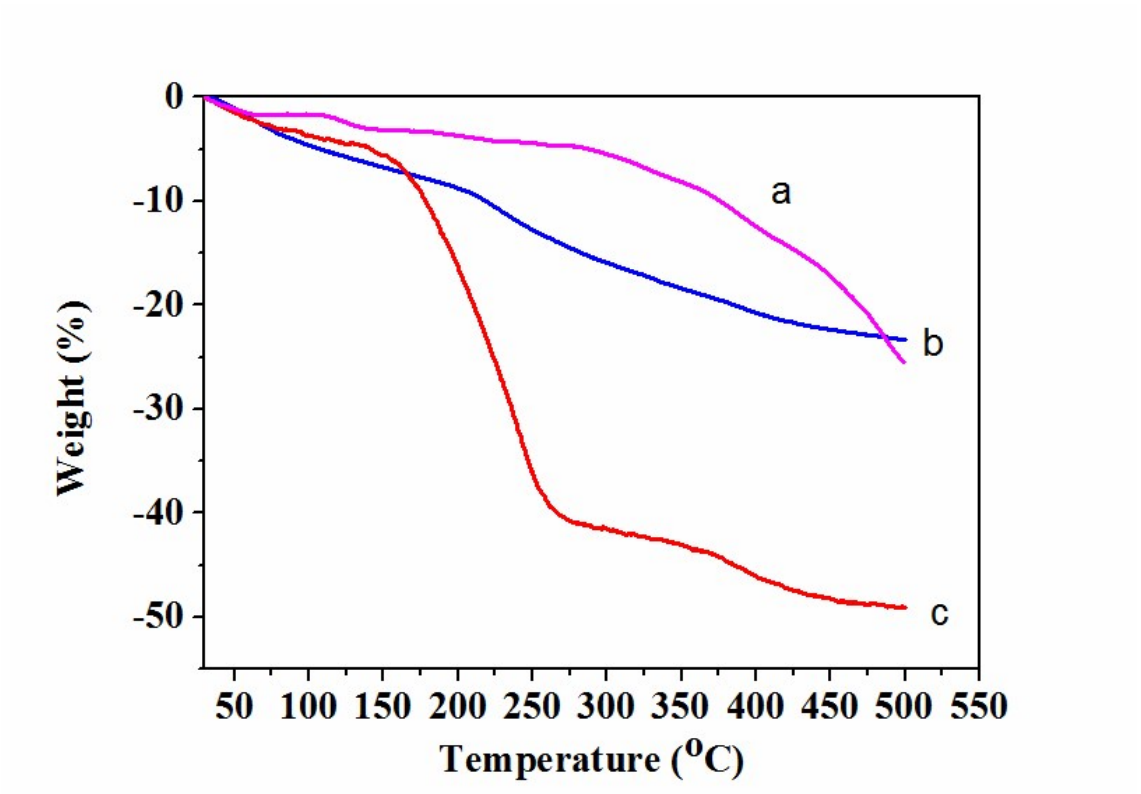

Fig. S17. TGA of (**a**) Ru@Z8, (**b**) Ru@Z8@SiO_2 and (**c**) Ru@CTAB@SiO_2 at a ramp rate of 2 ^{o}C min^{-1} under an Ar flow.

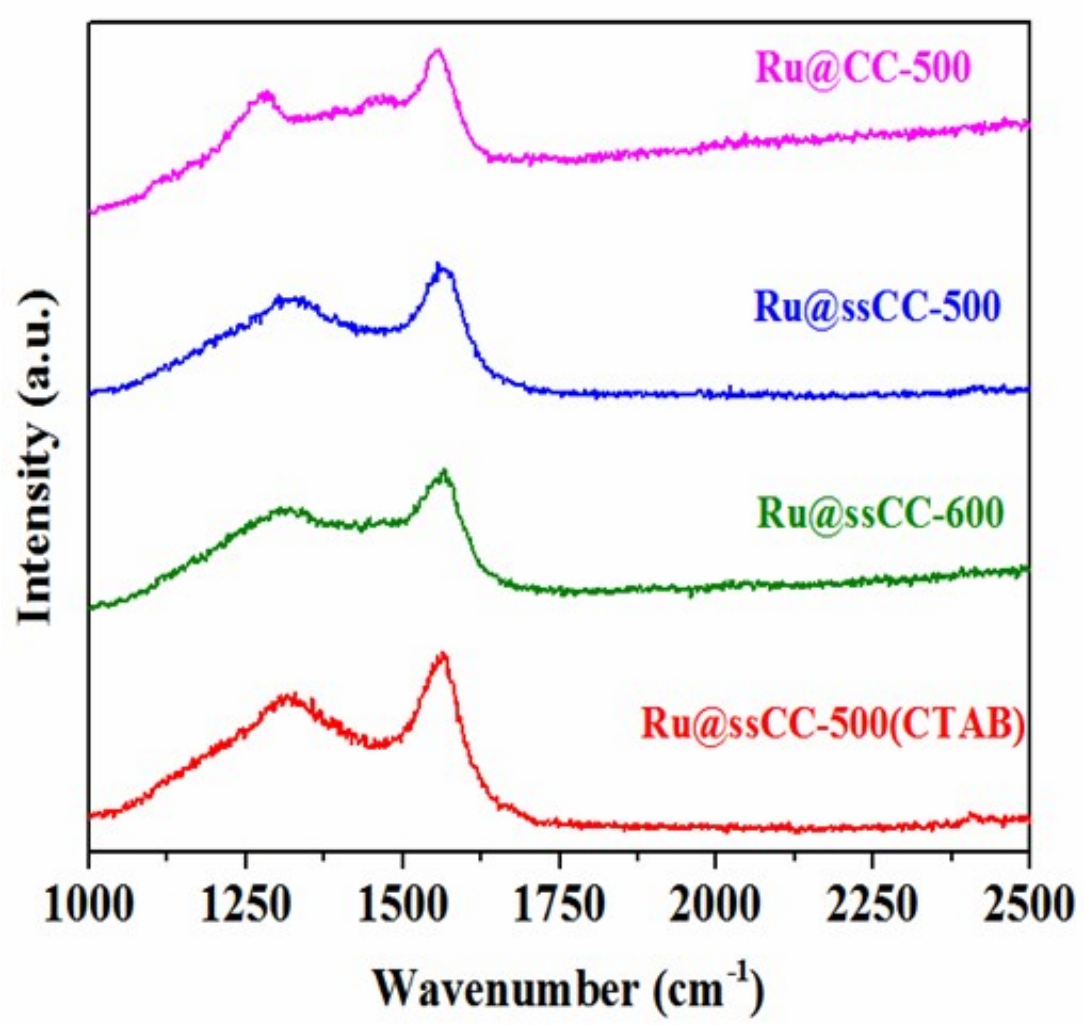

Fig. S18. Raman spectra of the Ru@CC-500, Ru@ssCC-500, Ru@ssCC-600 and Ru@ssCC-500(CTAB) catalysts.

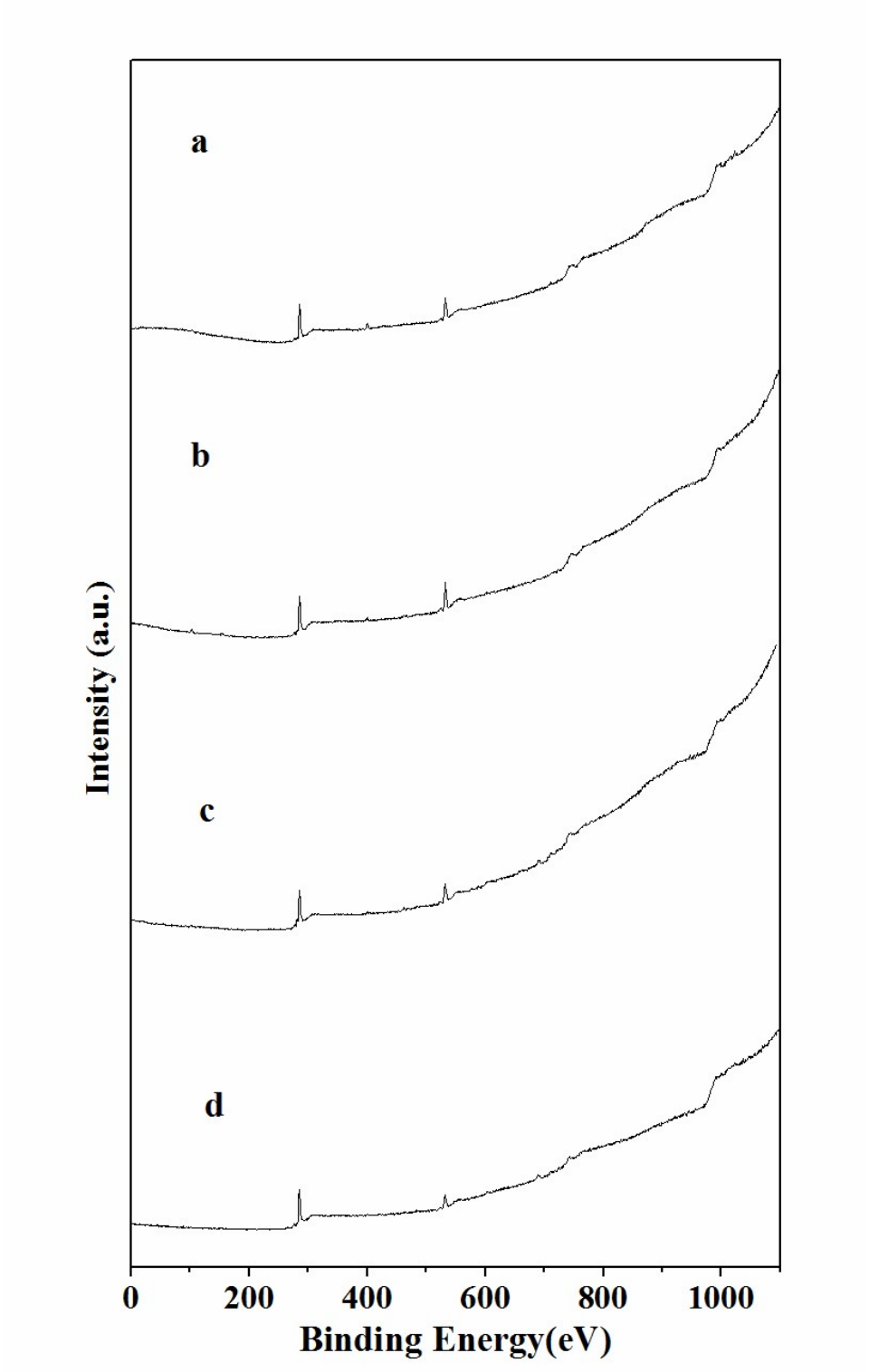

Fig. S19. XPS survey scans of the (**a**) Ru@CC-500, (**b**) Ru@ssCC-500, (**c**) Ru@ssCC-600 and (**d**) Ru@ssCC-500(CTAB) catalysts.

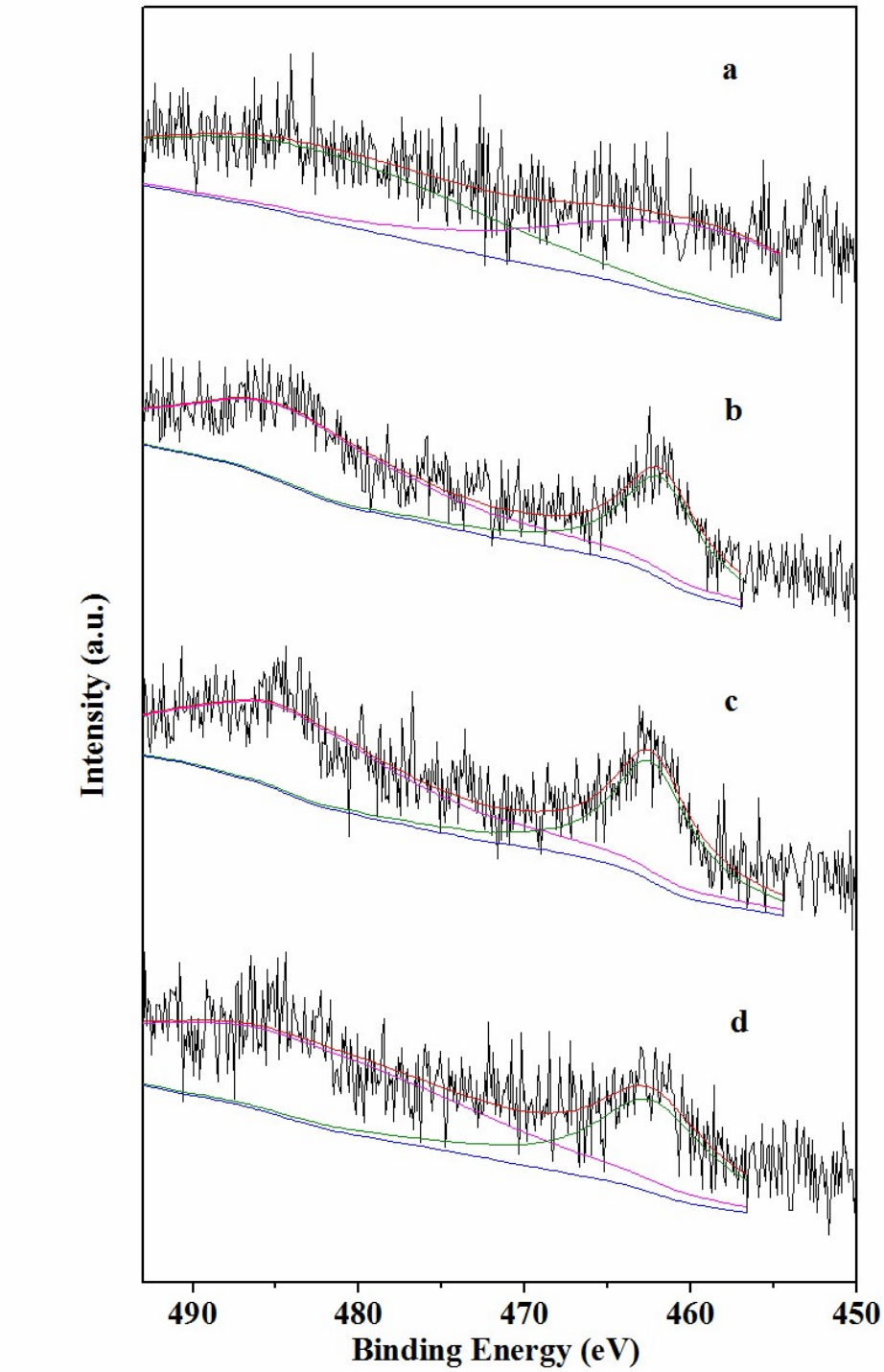

Fig. S20. Ru 3p spectra of the (**a**) Ru@CC-500, (**b**) Ru@ssCC-500, (**c**) Ru@ssCC-600 and (**d**) Ru@ssCC-500(CTAB) catalysts.

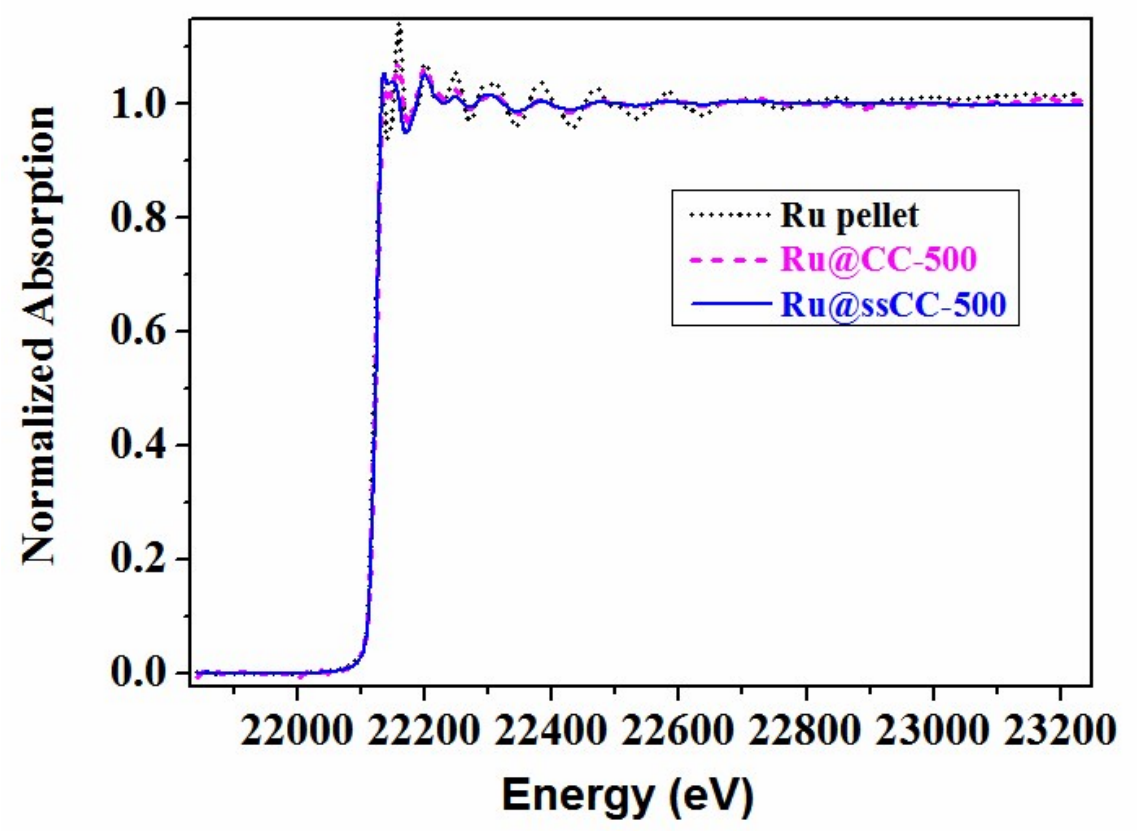

Fig. S21. Ru K-edge XAS spectra for Ru pellet, Ru@CC-500 and Ru@ssCC-500.

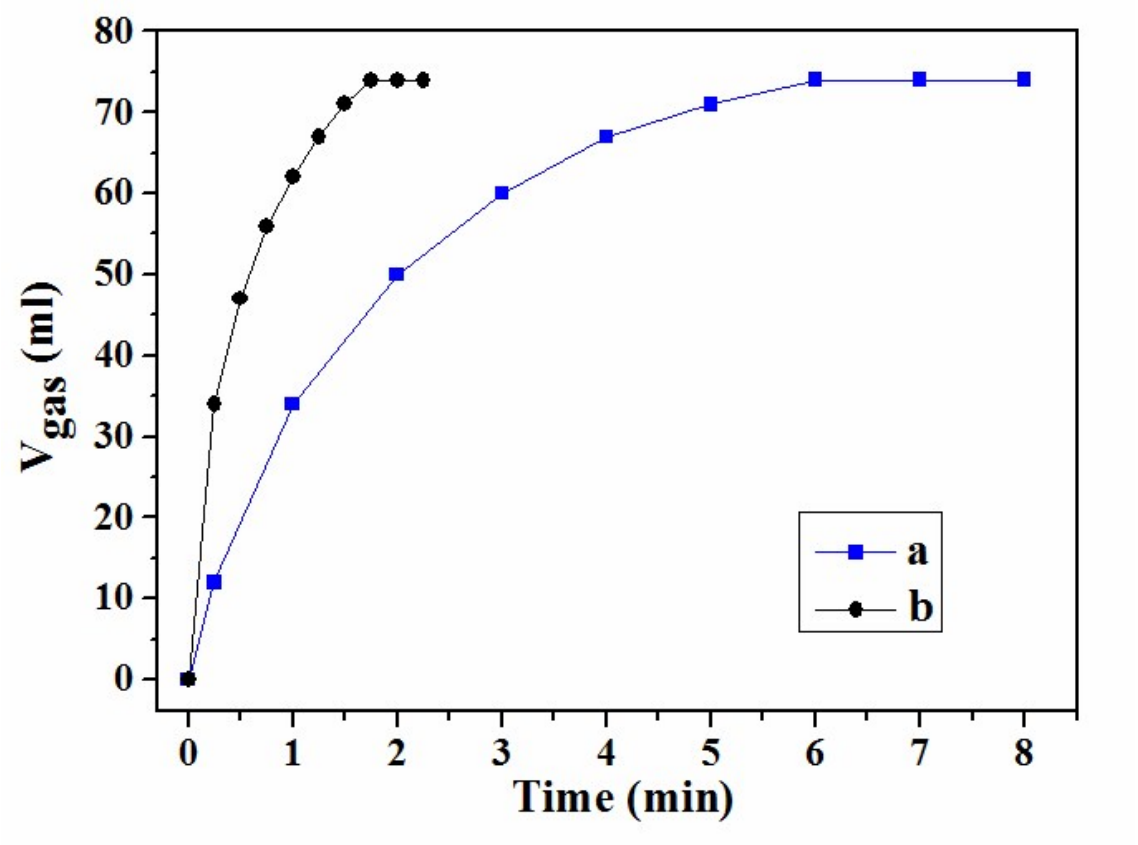

Fig. S22. Time course plots for the decomposition of H_2O_2 over the Ru@ssCC-500 catalysts at 303 K, $V_{(H2O)}$ = 3 mL, (**a**) $n_{(Ru)}/n_{(H2O2)} = 8.3 \times 10^{-5}$, (**b**) $n_{(Ru)}/n_{(H2O2)} = 2.5 \times 10^{-4}$.

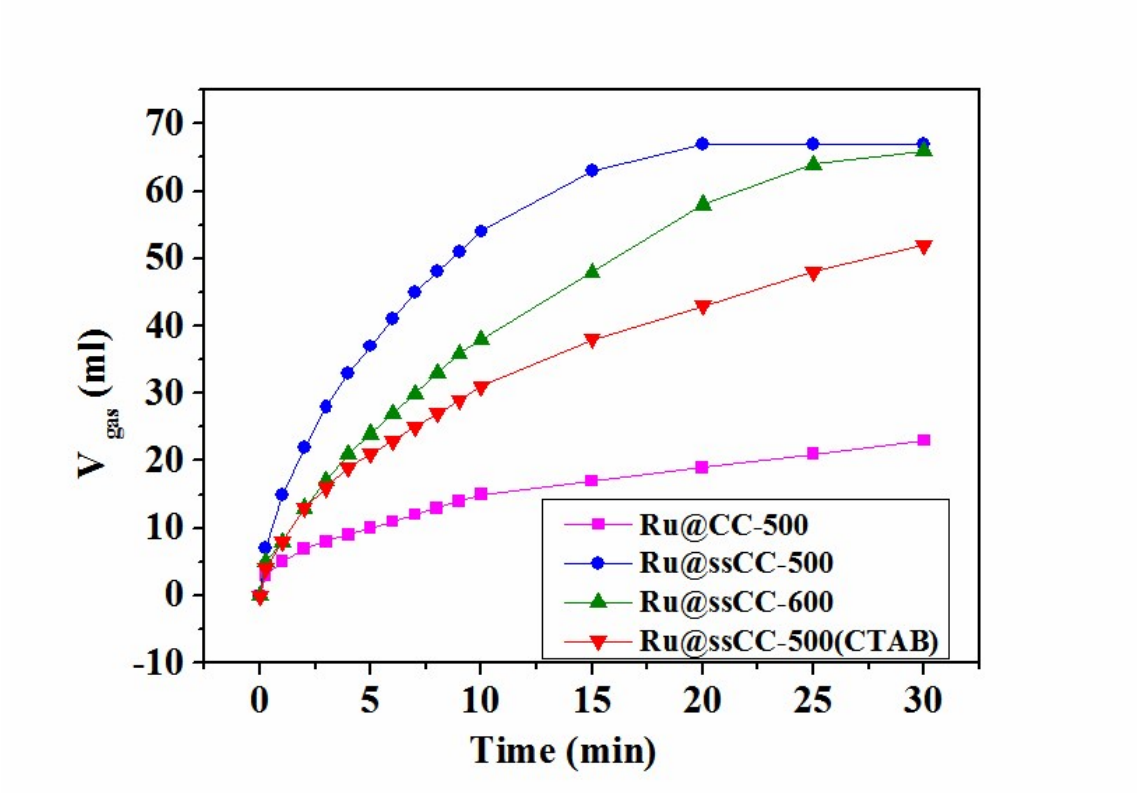

Fig. S23. Time course plots for the methanolysis of AB over the Ru@CC-500, Ru@ssCC-500, Ru@ssCC-600 and Ru@ssCC-500(CTAB) catalysts at 303 K ($n_{(Ru)}/n_{(AB)}$ = 5.0 × 10^{-4}, $V_{(methanol)}$ = 3 mL).

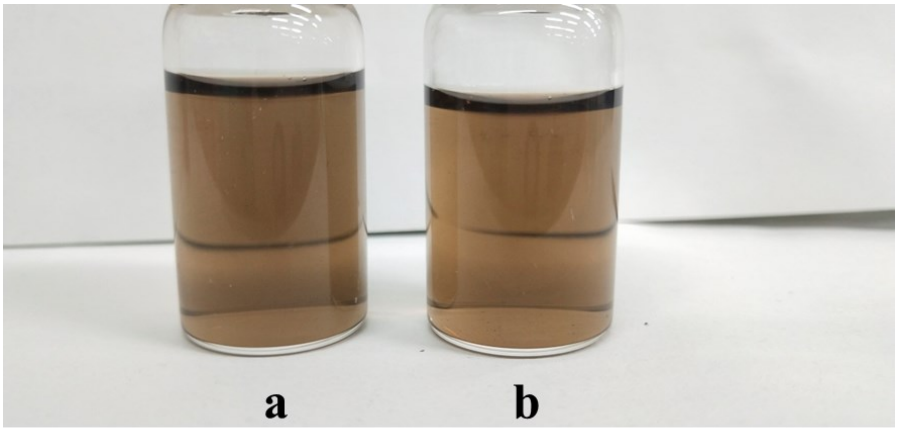

Fig. S24. Photographs of (**a**) Ru@ssCC-500 and (**b**) Ru@ssCC-500 recycled in water.

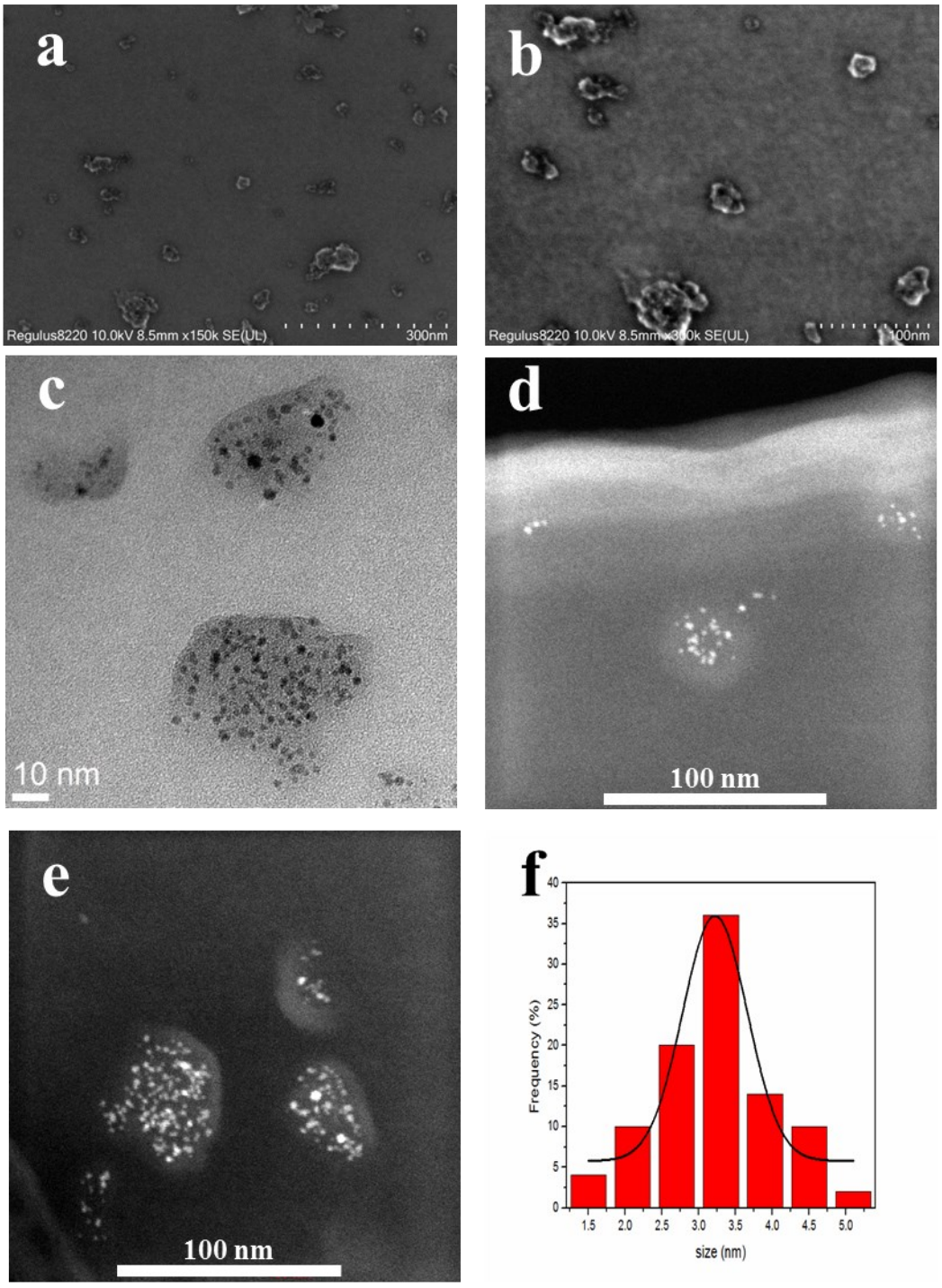

Fig. S25. (**a, b**) SEM, (**c**) TEM and (**d, e**) HAADF-STEM images, (**f**) particle size distribution histogram of the Ru nanoparticles on Ru@ssCC-500 recycled.

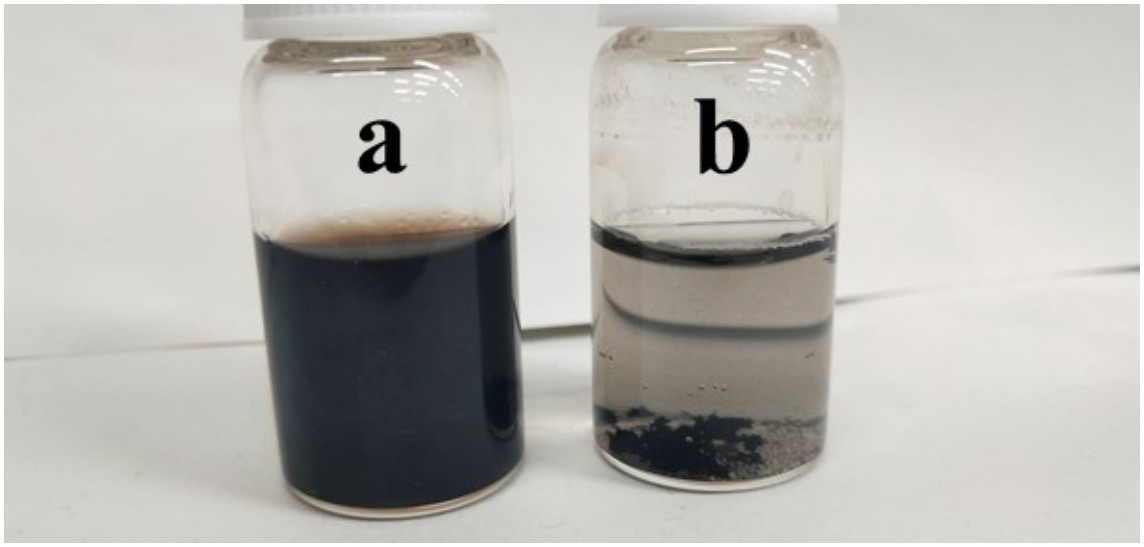

Fig. S26. Photographs of (**a**) $RuCl_3$ in H_2O, and (**b**) the Ru-SP-free catalyst obtained by reduction of $RuCl_3$.

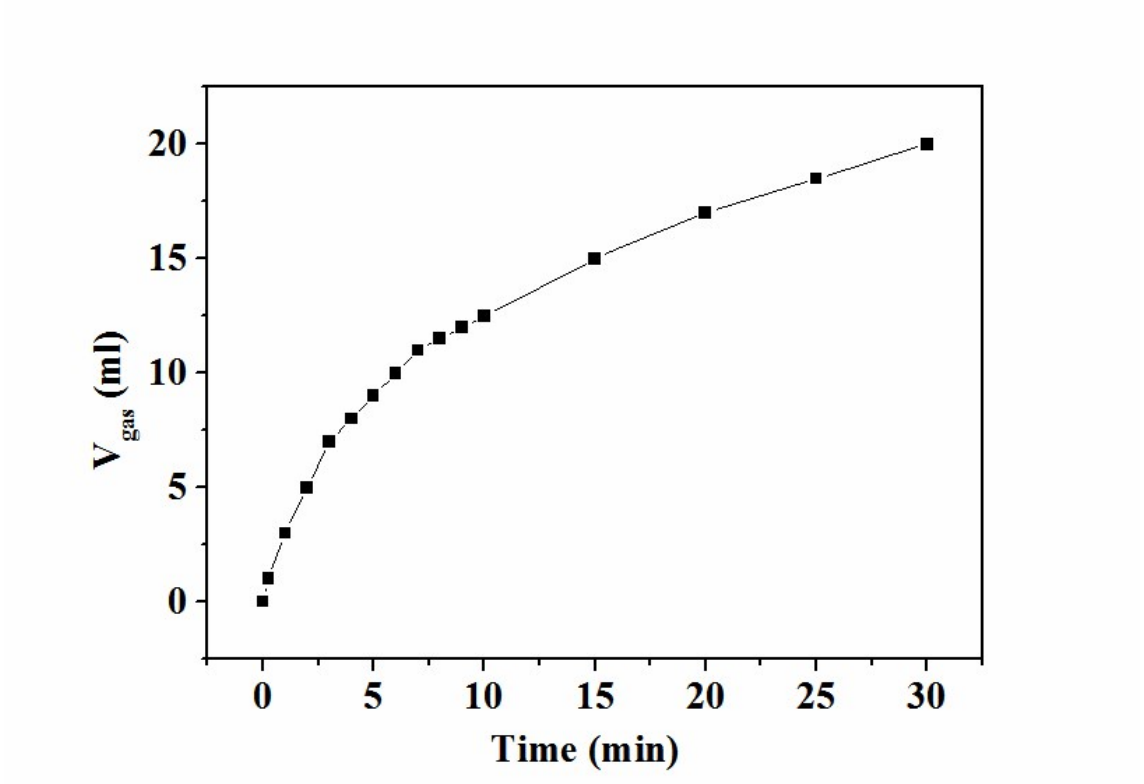

Fig. S27. Time course plots for the decomposition of H_2O_2 over the Ru-SP-free catalyst at 303 K ($n_{(Ru)}/n_{(H2O2)} = 8.3 \times 10^{-5}$, $V_{(H2O)} = 3$ mL).

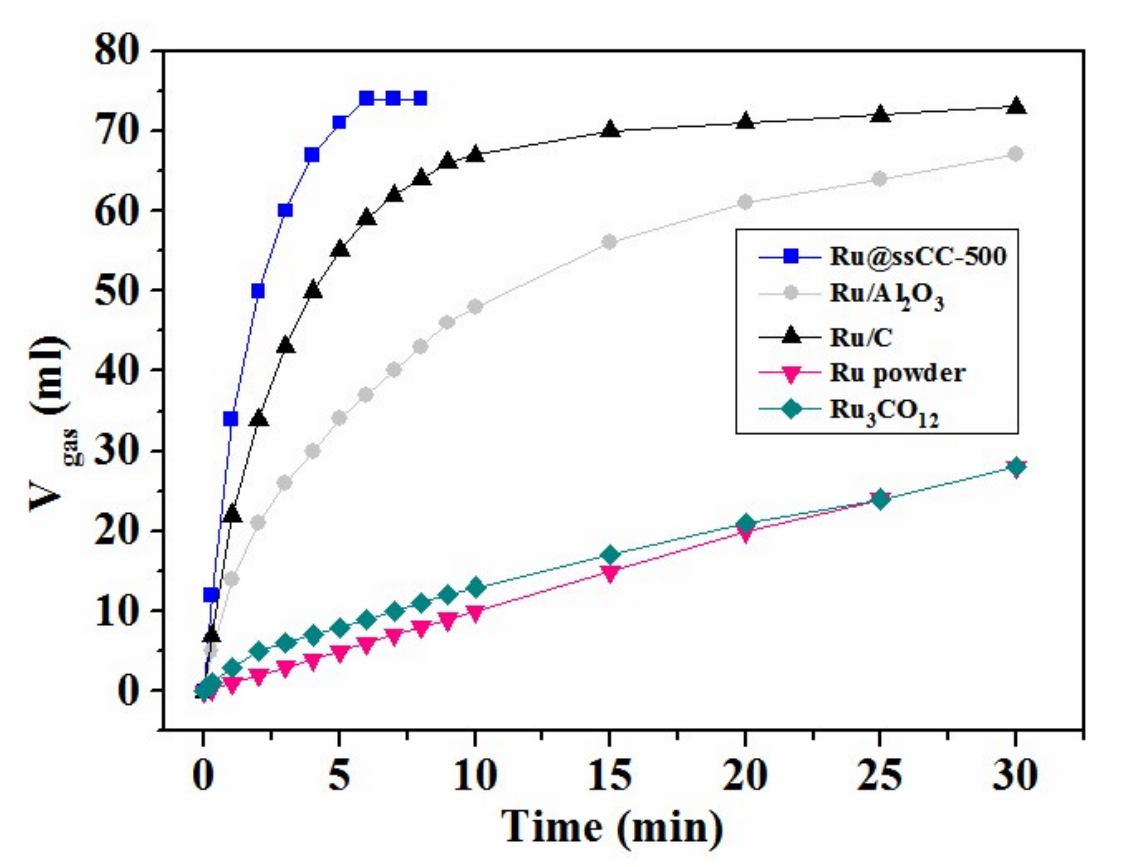

Fig. S28. Time course plots for the decomposition of H_2O_2 over the Ru@ssCC-500, Ru/Al_2O_3, Ru/C, Ru powder and Ru_3CO_{12} catalysts at 303 K ($n_{(Ru)}/n_{(H2O2)}$ = 8.3 × 10^{-5}, $V_{(H2O)}$ = 3 mL).

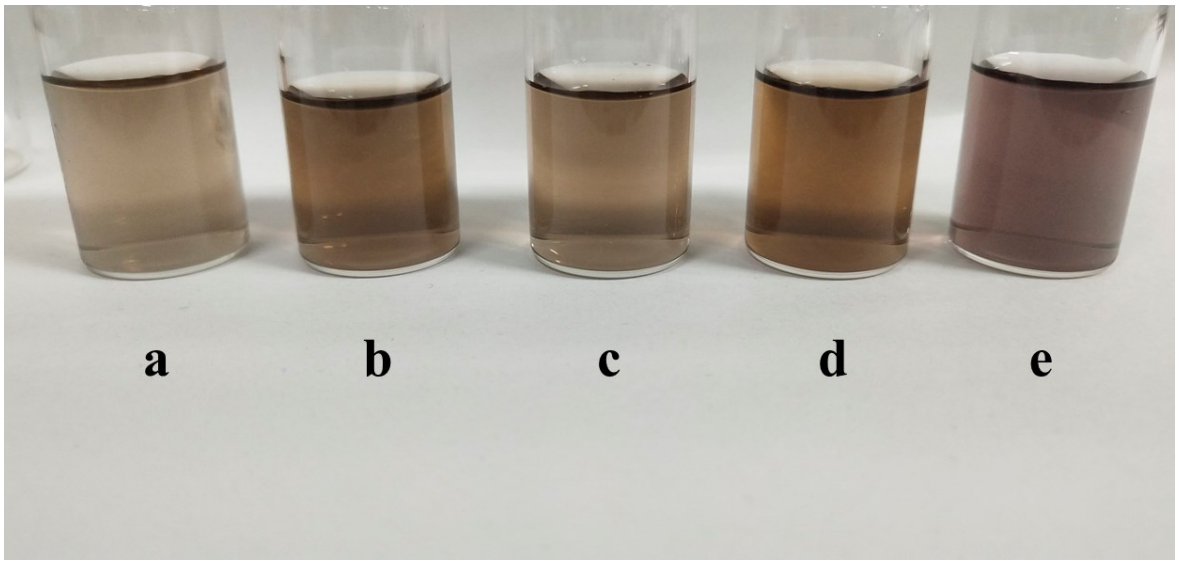

Fig. S29. Photographs of the (**a**) ssCC-500, (**b**) Pd@ssCC-500, (**c**) Pt@ssCC-500, (**d**) Rh@ssCC-500 and (**e**) Au@ssCC-500 catalysts in water.

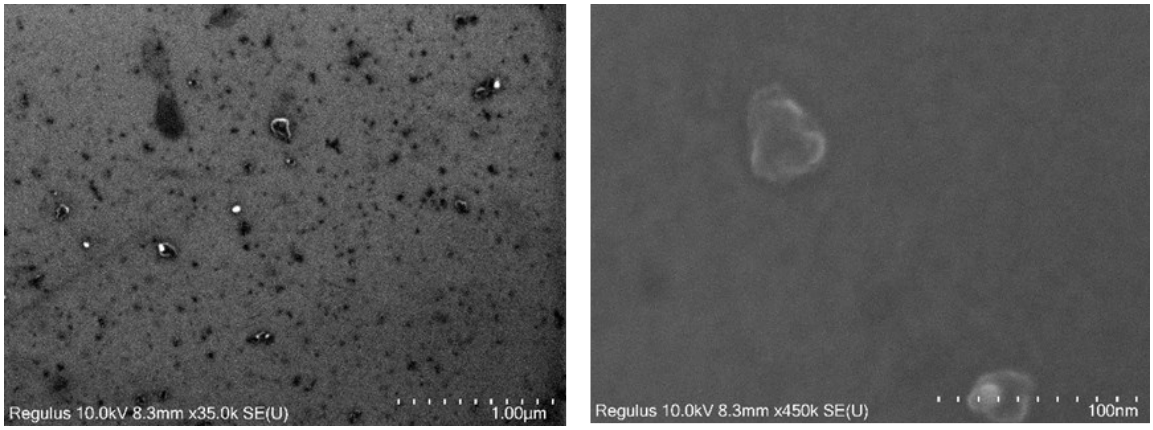

Fig. S30. SEM images of the Au@ssCC-500 catalysts.

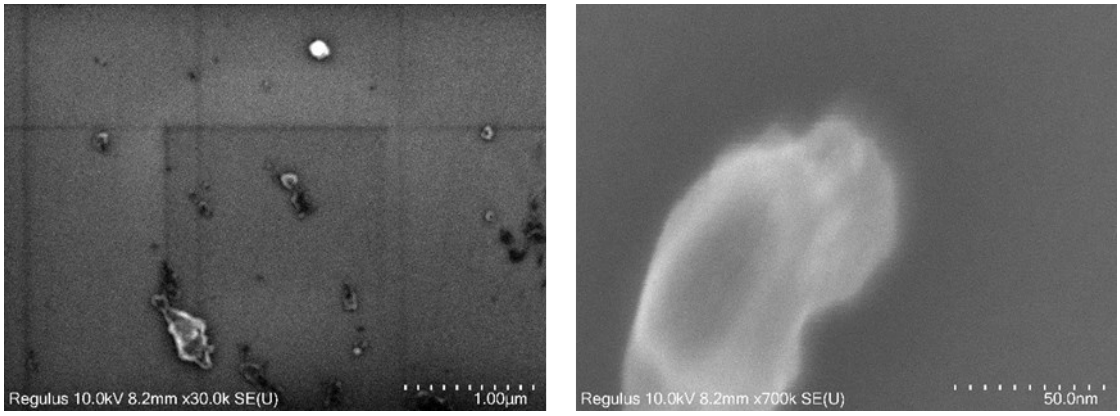

Fig. S31. SEM images of the Pd@ssCC-500 catalysts.

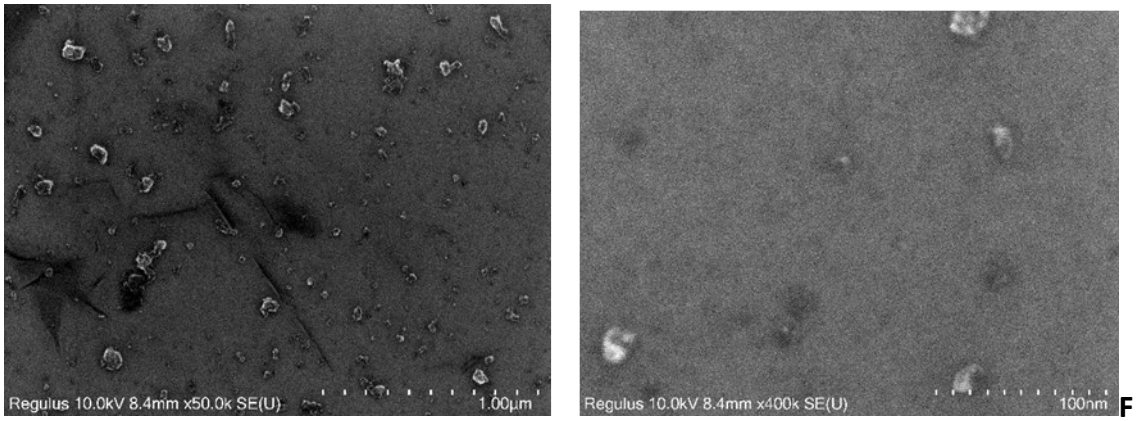

Fig. S32. SEM images of the Pt@ssCC-500 catalysts.

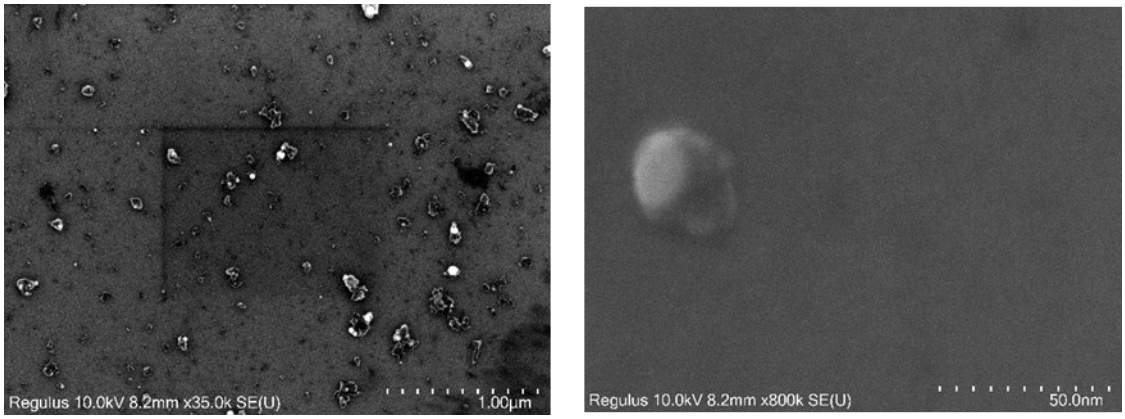

Fig. S33. SEM images of the Rh@ssCC-500 catalysts.

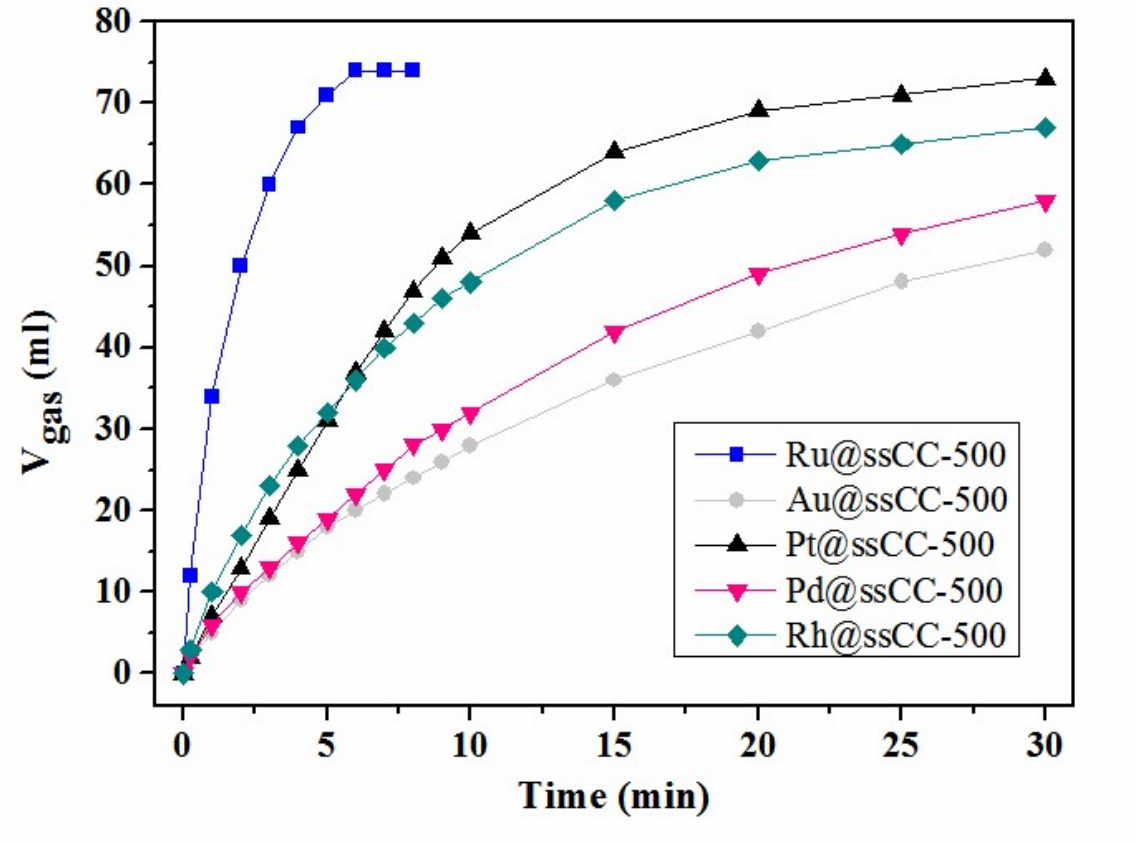

Fig. S34. Time course plots for the decomposition of H_2O_2 over the Ru@ssCC-500, Au@ssCC-500, Pt@ssCC-500, Pd@ssCC-500 and Rh@ssCC-500 catalysts at 303 K ($n_{(metal)}/n_{(H2O2)} = 8.3 \times 10^{-5}$, $V_{(H2O)} = 3$ mL).

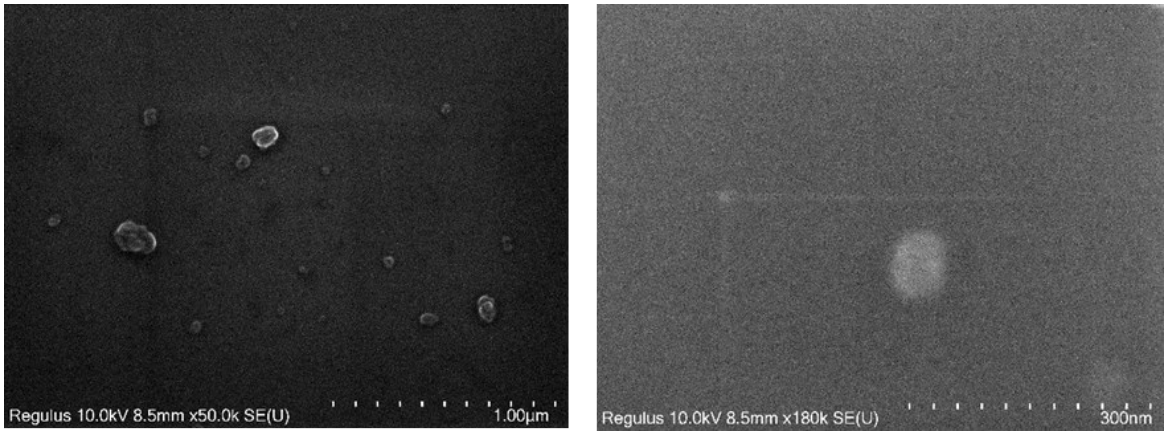

Fig. S35. SEM images of the ssCC@500 catalyst.

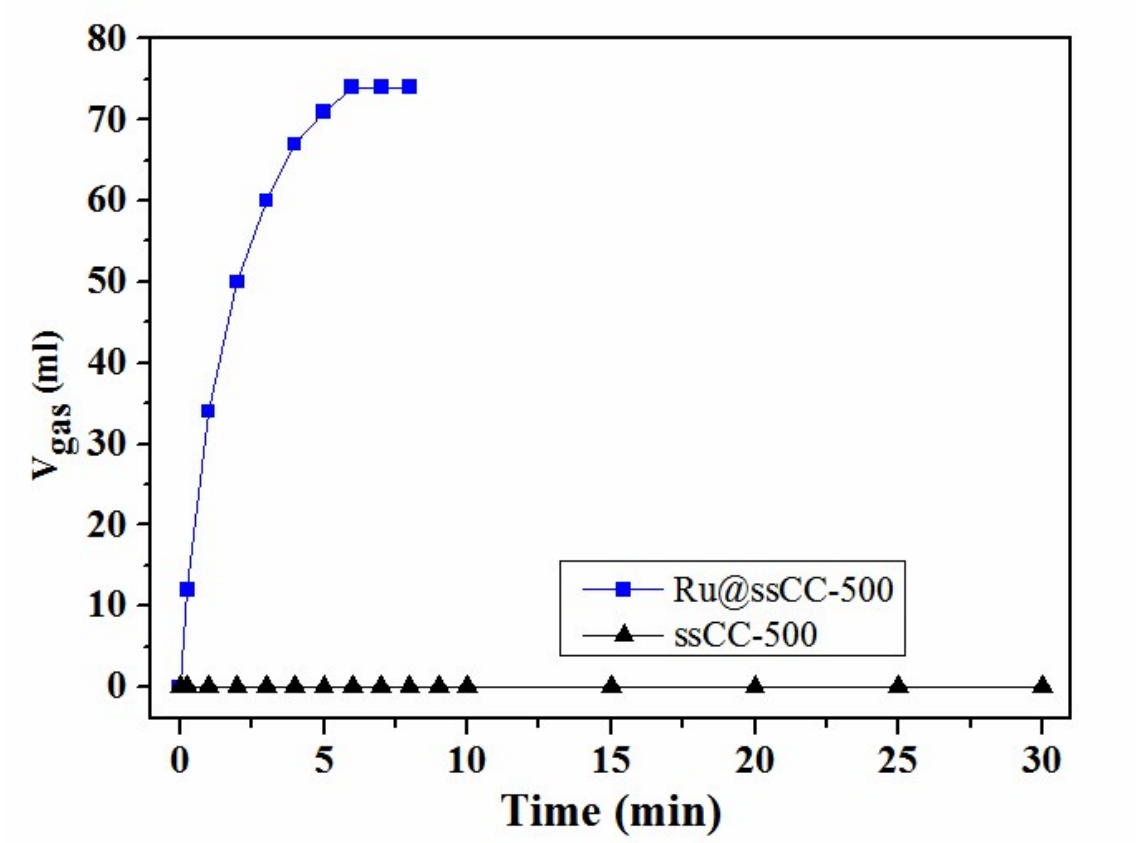

Fig. S36. Time course plots for the decomposition of H_2O_2 over the Ru@ssCC-500 and ssCC-500 catalysts at 303 K ($n_{(Ru)}/n_{(H2O2)} = 8.3 \times 10^{-5}$, $V_{(H2O)} = 3$ mL).

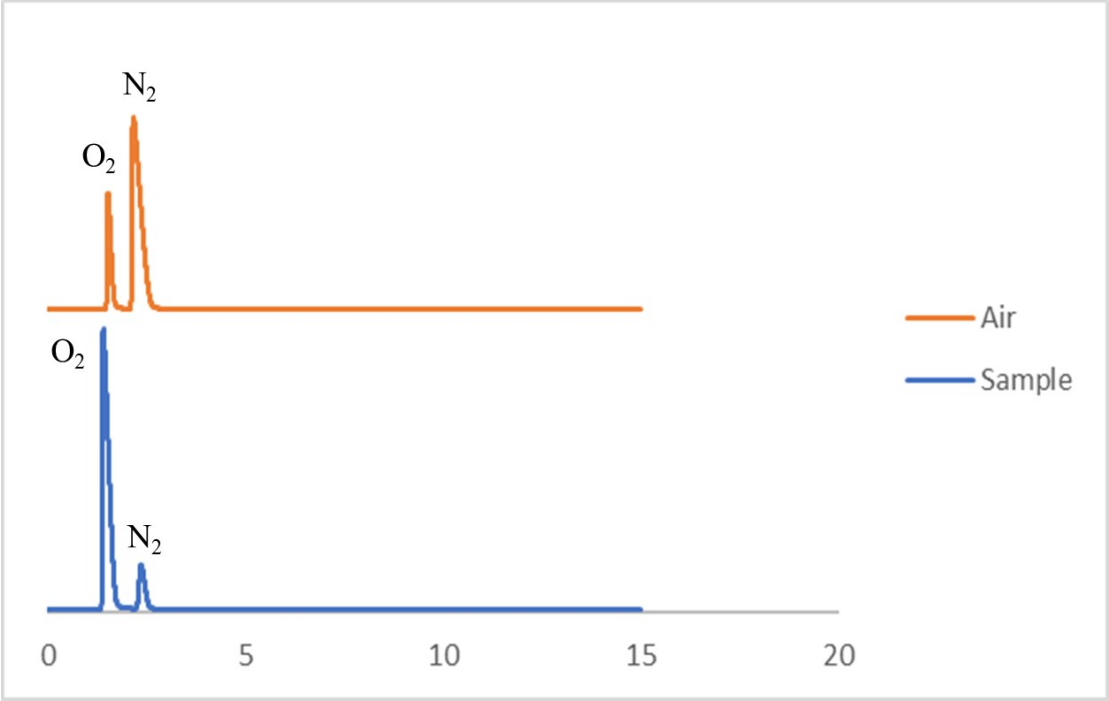

Fig. S37. Gas chromatograms of the released gas from the decomposition of H_2O_2 in the presence of the Ru@ssCC-500 catalyst.

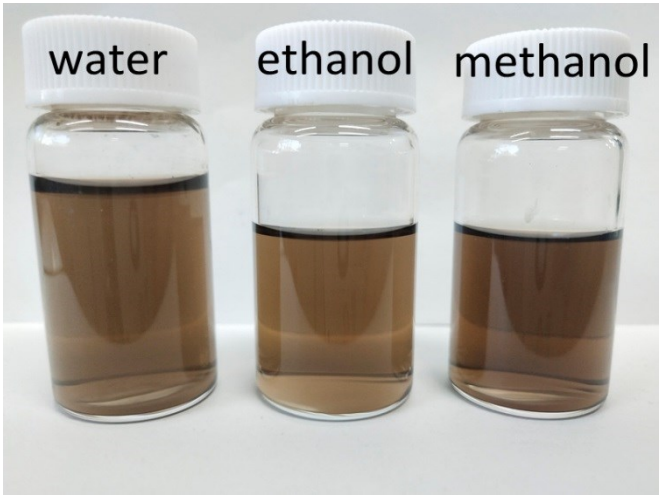

Fig. S38. The photograph of Ru@ssCC-500 dispersed in water/ethanol/methanol after 6 months of sitting.

Table S1. Ru contents of the catalysts.

	Samples	Ru (wt%)
1	Ru@CC-500	2.5
2	Ru@ssCC-500	5.0

Table S2. Atomic mass ratios of C, H and N in the catalysts.

	Samples	H (wt%)	C (wt%)	N (wt%)
1	Ru@CC-500	3.94	45.48	23.42
2	Ru@ssCC-500	3.66	43.35	19.58

Table S3. Binding energies and FWHM for C 1s of catalysts in Figure 2.

Samples	C=C (sp^2)		C-C (sp^3)		C-OH		C-O		C(O)OH	
	B.E. (eV)	FWHM (eV)	B.E. (eV)	FWHM (eV)	B.E. (eV)	FWHM (eV)	B.E. (eV)	FWHM (eV)	B.E. (eV)	FWHM (eV)
Ru@CC-500	284.8	1.5	285.5	1.7	/	/	286.8	2.0	288.7	1.9
Ru@ssCC-500	284.8	1.5	285.5	1.7	286.1	2.0	286.8	2.0	288.7	1.9
Ru@ssCC-600	284.8	1.6	285.6	1.8	/	/	286.7	2.0	288.6	2.0
Ru@ssCC-500(CTAB)	284.8	1.6	285.5	1.8	/	/	286.8	2.0	289.2	2.0

Table S4. Binding energies and FWHM for N 1s of catalysts in Figure 2.

Samples	Pyridinic N		Pyridonic N		Graphitic N	
	B.E. (eV)	FWHM (eV)	B.E. (eV)	FWHM (eV)	B.E. (eV)	FWHM (eV)
Ru@CC-500	398.9	2.0	400.2	2.0	401.4	2.0
Ru@ssCC-500	398.9	2.0	400.2	2.0	401.4	2.0
Ru@ssCC-600	398.9	2.0	400.2	2.0	401.5	2.0

Table S5. Binding energies and FWHM for O 1s of catalysts in Figure 2.

Samples	Adsorbed O		C=O		-OH		C-O	
	B.E. (eV)	FWHM (eV)	B.E. (eV)	FWHM (eV)	B.E. (eV)	FWHM (eV)	B.E. (eV)	FWHM (eV)
Ru@CC-500	530.1	1.4	531.5	2.0	532.5	1.9	534.2	2.0
Ru@ssCC-500	530.2	1.5	531.4	2.0	532.6	2.0	534.2	1.9
Ru@ssCC-600	530.1	1.5	531.4	1.9	532.4	2.1	534.1	1.9
Ru@ssCC-500(CTAB)	530.1	1.5	531.4	1.9	532.6	1.9	534.1	2.0

References

1. C. Wu, Q. Liu, R. Chen, J. Liu, H. Zhang, R. Li, K. Takahashi, P. Liu and J. Wang, *ACS Appl. Mater. Interfaces,* 2017, **9**, 11106-11115.
2. K. Lin, L. Chen, M. R. Prasad and C. Cheng, *Adv. Mater.,* 2004, **16**, 1845-1849.
3. Y. Chen, S. Ji, Y. Wang, J. Dong, W. Chen, Z. Li, R. Shen, L. Zheng, Z. Zhuang, D. Wang and Y. Li, *Angew. Chem., Int. Ed.,* 2017, **56**, 6937-6941.
4. H. Funke, A. C. Scheinost and M. Chukalina, *Physical Review B,* 2005, **71**, 094110.